

Review

# A Critical Review of Techniques for the Experimental Extraction of the Thermal Resistance of Bipolar Transistors from DC Measurements—Part I: Thermometer-Based Approaches

Vincenzo d’Alessandro <sup>1,\*</sup>, Antonio Pio Catalano <sup>1</sup>, Ciro Scognamillo <sup>1</sup>, Markus Müller <sup>2</sup>, Michael Schröter <sup>2</sup>, Peter J. Zampardi <sup>3</sup> and Lorenzo Codecasa <sup>4</sup>

<sup>1</sup> Department of Electrical Engineering and Information Technology, University Federico II, 80125 Naples, Italy; antoniopio.catalano@unina.it (A.P.C.); ciro.scognamillo@unina.it (C.S.)

<sup>2</sup> Chair for Electron Devices and Integrated Circuits, TU Dresden, 01069 Dresden, Germany; markus.mueller3@tu-dresden.de (M.M.); mschroter@ieee.org (M.S.)

<sup>3</sup> Qorvo, Inc., Newbury Park, CA 91320, USA; peter.zampardi@qorvo.com

<sup>4</sup> Department of Electronics, Information, and Bioengineering, Politecnico di Milano, 20133 Milan, Italy; lorenzo.codecasa@polimi.it

\* Correspondence: vindales@unina.it

**Abstract:** This paper presents a critical and detailed overview of experimental techniques for the extraction of the thermal resistance of bipolar transistors from simple DC current/voltage measurements. More specifically, this study focuses on techniques based on a thermometer, i.e., the relation between the base-emitter voltage and the junction temperature. The theory behind the techniques is described with a unified and comprehensible nomenclature. Advantages, underlying approximations, and limitations of the methods are illustrated. The accuracy is assessed by emulating the DC measurements with PSPICE electrothermal simulations of a transistor model, applying the techniques to the simulated currents/voltages, and comparing the extracted thermal resistance data with the values obtained from the target formulation embedded in the transistor model. An InGaP/GaAs HBT and an Si/SiGe HBT for high-frequency applications are considered as case-studies.

**Keywords:** bipolar transistor model; gallium arsenide (GaAs); heterojunction bipolar transistor (HBT); nonlinear thermal effects; silicon-germanium (SiGe); thermal resistance



**Citation:** d’Alessandro, V.; Catalano, A.P.; Scognamillo, C.; Müller, M.; Schröter, M.; Zampardi, P.J.; Codecasa, L. A Critical Review of Techniques for the Experimental Extraction of the Thermal Resistance of Bipolar Transistors from DC Measurements—Part I: Thermometer-Based Approaches. *Electronics* **2023**, *12*, 3471. <https://doi.org/10.3390/electronics12163471>

Academic Editor: Frédérique Ducroquet

Received: 11 July 2023

Revised: 12 August 2023

Accepted: 13 August 2023

Published: 16 August 2023



**Copyright:** © 2023 by the authors. Licensee MDPI, Basel, Switzerland. This article is an open access article distributed under the terms and conditions of the Creative Commons Attribution (CC BY) license (<https://creativecommons.org/licenses/by/4.0/>).

## 1. Introduction

Electrothermal (ET) effects plague modern high-frequency bipolar transistors in multiple ways, as they can lead to distortion in the I–V curves, which modifies the DC bias and shrinks the safe operating area [1–4], degradation of the small-signal low-frequency behavior [5,6], reduction in cut-off frequency caused by the higher scattering rate [7], and even irreversible failure, likely to occur in multifinger devices due to thermally-induced current hogging [8–11]. This holds true regardless of the technology and is dictated by the high operating current (and power) densities and the high self-heating thermal resistances. In gallium arsenide (GaAs)-based heterojunction bipolar transistors (HBTs) like InGaP/GaAs and AlGaAs/GaAs, considered the dominant technology for handset power amplifier design, the high thermal resistances are a consequence of (i) the low thermal conductivity of the GaAs substrate (one third of that of silicon), (ii) the lateral heat confinement due to mesa isolation, and (iii) the interlevel dielectric films [9,10,12–15]. In silicon/silicon-germanium (Si/SiGe) HBTs for mm-wave and near-THz applications, namely, wireless and optical communication, medical equipment, and automotive radars, the increase in thermal resistances is due to technology strategies devised to boost the frequency performance, like (i) adoption of oxide-based shallow/deep trenches and reduction of the spacing between intrinsic transistor and trenches, which hinder the lateral heat propagation from the power dissipation region, and (ii) horizontal scaling of the emitter, which drives higher current

(and power) density; such factors have contributed to push the thermal resistances of single-finger HBTs into the thousands of K/W [16–22].

In a bipolar transistor, the thermal resistance  $R_{TH}$  [K/W] is defined as the ratio between the temperature rise  $\Delta T_j = T_j - T_B$  [K] divided by the dissipated power  $P_D$  [W], where  $T_j$  [K] is the temperature averaged over the base-emitter junction and  $T_B$  [K] is the backside temperature. This definition is reasonable since the electrical characteristics of the device markedly depend on  $T_j$ . Accurately assessing the thermal resistance from experimental data is of utmost importance in terms of thermal characterization, modeling/simulation for device/circuit design, as well as reliability estimation.

In general, there are *two* experimental approaches for assessing the temperature of a transistor: the *direct* one is based on the detection of temperature maps over the top surface of the exposed chip (through e.g., infrared imaging and liquid crystal methods), while the *indirect* one relies on the measurement of currents/voltages and only allows determining a single temperature value in a relevant device region. For downscaled bipolar transistors for high-frequency applications, indirect techniques are the common choice, as direct methods can only detect the temperature over the top surface (the base-emitter junction is not exposed) and suffer from limited space resolution. As a result, a single “average”  $T_j$  value is *indirectly* extracted, but this does not represent a problem for aggressively scaled devices, in which the base-emitter temperature is expected to be almost uniform. Within the realm of indirect techniques, those based on DC measurements are often preferred to low-frequency AC or pulsed transient methods, since they are easier to perform and require cheaper equipment. DC indirect techniques can be in turn subdivided into the following categories.

- Techniques using a *thermometer*, i.e., the relation between a temperature-sensitive electrical parameter (TSEP) and the temperature in a relevant device region [18,23–31]. The TSEP typically adopted in a bipolar transistor is the base-emitter voltage  $V_{BE}$ , as it varies with temperature more linearly than the common-emitter forward current gain  $\beta_F$  [24].
- Techniques exploiting intersection points [20,22,32–34].
- Techniques based on the measurement of the base current  $I_B$  [35–39].
- A technique relying on analytical assumptions that allows the full evaluation of nonlinear thermal effects [40].

A review of all the above methods has been recently published [41], which clarifies that none of them can be considered the absolute best, as the accuracy of each technique depends on specific circumstances (biasing conditions and technology under test).

This paper critically investigates and compares only thermometer-based DC indirect techniques, while follow-up papers will be dedicated to other approaches. The work is intended to extend and complete the analysis conducted in [41] by providing much more details on the theory on which the techniques are based, as well as on the reasons of extraction inaccuracy.

In Section 2, an extensive theoretical background is offered, which explains the temperature dependence of the collector current, gives the thermal resistance definition, and provides some details on nonlinear thermal effects. Section 3 presents the devices selected as case-studies and probes into the circuit-based simulation approach needed to analyze the accuracy of the techniques of interest. Section 4 describes the theory behind the techniques in a tutorial style with a unified and comprehensible nomenclature, clarifies advantages, limitations, and approximations, draws simple guidelines for their correct applications, shows and discusses the results. Conclusions are finally given in Section 5.

## 2. Theoretical Background

### 2.1. Temperature Dependence of the Collector Current

The collector current  $I_C$  of a bipolar transistor operated in forward active mode can be expressed as

$$I_C = M \cdot I_{CT} \quad (1)$$

where  $M (\geq 1)$  is the dimensionless  $V_{CB}$ -dependent avalanche multiplication factor,  $V_{CB}$  [V] being the collector-base voltage, and  $I_{CT}$  [A] ( $\approx I_E$ , emitter current) represents the minority transport current flowing across the quasi-neutral base region [42].  $I_{CT}$  is given by

$$I_{CT} = \left(1 + \frac{V_{CB}}{V_{AF}}\right) \cdot \frac{1}{B_{HI}} \cdot \frac{q \cdot A_E \cdot D_{nB}(T_j) \cdot n_{iB}^2(T_j)}{W_B \cdot N_B} \cdot \exp\left(\frac{V_{BEj}}{\eta \cdot V_T}\right) \quad (2)$$

where

- $V_{AF}$  [V] is the forward Early voltage;
- $B_{HI} (\geq 1)$  is an  $I_C$ -dependent dimensionless term included to empirically describe the attenuation dictated by high-injection (high-current) effects leading to the gain roll-off;
- $q$  [C] is the absolute value of the electron charge (or *elementary charge*);
- $A_E$  [cm<sup>2</sup> or  $\mu\text{m}^2$ ] is the emitter area;
- $T_j$  [K] is the average temperature over the base-emitter junction (also simply referred to as *junction temperature*), as mentioned in Section 1;
- $D_{nB}$  [cm<sup>2</sup>/s] is the average electron diffusivity in the quasi-neutral base region;
- $n_{iB}$  [cm<sup>-3</sup>] is the intrinsic carrier concentration in the base;
- $W_B$  [cm or  $\mu\text{m}$ ] is the quasi-neutral base width;
- $N_B$  [cm<sup>-3</sup>] is the average base doping;
- $V_{BEj}$  [V] is the “internal” (junction) base-emitter voltage, that is,  $V_{BEj} = V_{BE} - R_B \cdot I_B - R_E \cdot I_E$ , where  $V_{BE}$  [V] is the externally-accessible base-emitter voltage,  $I_B$  and  $I_E$  [A] are the base and emitter current, respectively, and  $R_B$  and  $R_E$  [ $\Omega$ ] are the parasitic base and emitter resistances, respectively;
- $\eta$  is the dimensionless ideality coefficient;
- $V_T = kT_j/q$  [V] is the thermal voltage at  $T_j$ ,  $k = 8.617 \times 10^{-5}$  eV/K being the Boltzmann constant.

Using the Einstein relation,  $D_{nB}$  can be expressed as

$$D_{nB}(T_j) = V_T \cdot \mu_{nB}(T_j) = \frac{kT_j}{q} \cdot \mu_{nB}(T_0) \cdot \left(\frac{T_j}{T_0}\right)^{-m_B} \quad (3)$$

where  $T_0 = 300$  K is the reference temperature,  $\mu_{nB}$  [cm<sup>2</sup>/Vs] is the electron mobility, and  $m_B (>0)$  is a doping-dependent power factor. Moreover,

$$n_{iB}^2(T_j) = A \cdot T_j^3 \cdot \exp\left[-\frac{E_G(T_j) - \Delta E_{GB}}{kT_j}\right] = A \cdot T_j^3 \cdot \exp\left[-\frac{V_G(T_j) - \Delta V_{GB}}{kT_j/q}\right] \quad (4)$$

where  $A$  is a temperature-insensitive term,  $E_G$  [eV] is the bandgap of the base semiconductor,  $\Delta E_{GB}$  [eV] is a potential bandgap narrowing (e.g., due to heavy doping or presence of a Ge mole fraction), and  $V_G$  and  $\Delta V_{GB}$  are the voltage equivalents of  $E_G$  and  $\Delta E_{GB}$ , respectively. Since for temperatures higher than 250 K  $V_G(T_j)$  can be reasonably approximated by

$$V_G(T_j) \approx V_{G0} - \chi \cdot T_j \quad (5)$$

where  $V_{G0} = 1.21$  V and  $\chi = 2.85 \times 10^{-4}$  V/K for Si [43],  $V_{G0} = 1.57$  V and  $\chi = 4.85 \times 10^{-4}$  V/K for GaAs, (4) becomes

$$n_{iB}^2(T_j) = A \cdot \exp\left(\frac{\chi \cdot q}{k}\right) \cdot T_j^3 \cdot \exp\left(-\frac{V_{G0} - \Delta V_{GB}}{kT_j/q}\right) = B \cdot T_j^3 \cdot \left(-\frac{V_{G0} - \Delta V_{GB}}{kT_j/q}\right) \quad (6)$$

Using (2), (3) and (6), (1) turns into

$$\begin{aligned} I_C &= M(V_{CB}) \cdot \left(1 + \frac{V_{CB}}{V_{AF}}\right) \cdot \frac{1}{B_{HI}(I_C)} \cdot C \cdot T_j^{4-m_B} \cdot \exp\left(-\frac{V_{G0} - \Delta V_{GB}}{kT_j/q}\right) \cdot \exp\left(\frac{V_{BEj}}{\eta \cdot kT_j/q}\right) \\ &\approx M(V_{CB}) \cdot \left(1 + \frac{V_{CB}}{V_{AF}}\right) \cdot \frac{1}{B_{HI}(I_C)} \cdot C \cdot T_j^{4-m_B} \cdot \exp\left[\frac{V_{BEj} - (V_{G0} - \Delta V_{GB})}{\eta \cdot kT_j/q}\right] \end{aligned} \quad (7)$$

where C is a temperature- and bias-independent term.

From (7), it can be easily found that

$$V_{BEj} = V_{G0} - \Delta V_{GB} - \eta \cdot \frac{kT_j}{q} \cdot \ln \frac{M(V_{CB}) \cdot \left(1 + \frac{V_{CB}}{V_{AF}}\right) \cdot C \cdot T_j^{4-m_B}}{I_C \cdot B_{HI}(I_C)} \quad (8)$$

Let us now evaluate the (positive) temperature coefficient  $\phi$  [V/K] given by

$$\phi = - \left. \frac{\partial V_{BEj}}{\partial T_j} \right|_{I_C, V_{CB}} \quad (9)$$

which inherently assumes that  $T_j$  increases by varying  $T_B$ . From (8),

$$\begin{aligned} \phi &= \eta \cdot \frac{k}{q} \cdot (4 - m_B) - \eta \cdot \frac{k}{q} \cdot \ln \frac{I_C \cdot B_{HI}(I_C)}{M(V_{CB}) \cdot \left(1 + \frac{V_{CB}}{V_{AF}}\right) \cdot C \cdot T_j^{4-m_B}} \\ &= \eta \cdot \frac{k}{q} \cdot (4 - m_B) + \eta \cdot \frac{k}{q} \cdot \ln \frac{C \cdot T_j^{4-m_B}}{A_E \cdot J_{S0}} - \eta \cdot \frac{k}{q} \cdot \ln \frac{I_C \cdot B_{HI}(I_C)}{M(V_{CB}) \cdot \left(1 + \frac{V_{CB}}{V_{AF}}\right) \cdot A_E \cdot J_{S0}} \\ &\approx \eta \cdot \frac{k}{q} \cdot (4 - m_B) + \eta \cdot \frac{k}{q} \cdot \ln \frac{C \cdot T_0^{4-m_B}}{A_E \cdot J_{S0}} - \eta \cdot \frac{k}{q} \cdot \ln \frac{I_C \cdot B_{HI}(I_C)}{M(V_{CB}) \cdot \left(1 + \frac{V_{CB}}{V_{AF}}\right) \cdot A_E \cdot J_{S0}} = \phi_0 - \eta \cdot \frac{k}{q} \cdot \ln \frac{I_{CT0}}{A_E \cdot J_{S0}} \end{aligned} \quad (10)$$

where  $\phi_0 = \eta \cdot \frac{k}{q} \cdot \left[ (4 - m_B) + \ln \frac{C \cdot T_0^{4-m_B}}{A_E \cdot J_{S0}} \right]$  [V/K] is a bias- and almost-temperature-independent parameter (typically falling in the range 3 to 6 mV/K) [1,18],  $J_{S0}$  [A/cm<sup>2</sup> or A/μm<sup>2</sup>] is the reverse saturation current density at the reference temperature  $T_0$ , and  $I_{CT0}$  [A] is the collector current without avalanche, Early, and high-injection effects. Coefficient  $\phi$  does not markedly depend on the transistor layout (i.e., on  $A_E$ ).

Let us consider a practical case where the bipolar transistor is operated in a common-base configuration with an assigned  $I_E$  and assume that  $V_{CB}$  is kept low enough to avoid the avalanche effect ( $I_C = I_{CT} \approx I_E$ ) and that the device does not suffer from a significant Early effect. From (8) it is obtained that

$$V_{BEj} = V_{G0} - \Delta V_{GB} - \eta \cdot \frac{kT_j}{q} \cdot \ln \frac{C \cdot T_j^{4-m_B}}{I_E \cdot B_{HI}(I_E)} \quad (11)$$

If the junction temperature  $T_j$  is not higher than 400 K, (11) can be reasonably approximated as

$$V_{BEj} \approx V_{G0} - \Delta V_{GB} - \eta \cdot \frac{kT_j}{q} \cdot \ln \frac{C \cdot T_0^{4-m_B}}{I_E \cdot B_{HI}(I_E)} \quad (12)$$

which can be expressed as

$$V_{BEj} \approx V_{BEj}(T_0) - \phi \cdot (T_j - T_0) \quad (13)$$

where  $V_{BEj}(T_0) = V_{BEj}(T_j = T_0)$ . The temperature coefficient  $\phi = -\left.\frac{\partial V_{BEj}}{\partial T_j}\right|_{I_E}$ , calculated from (11), becomes

$$\phi = \phi_0 - \eta \cdot \frac{k}{q} \cdot \ln \frac{I_E \cdot B_{HI}(I_E)}{A_E \cdot J_{S0}} \tag{14}$$

From (13), it is clear that

- by increasing the backside (or baseplate, or ambient) temperature  $T_B$  through a thermochuck at given values of  $I_E$  and  $V_{CB}$ , the junction temperature  $T_j$  increases, and  $V_{BEj}$  decreases almost linearly with  $T_j$ ;
- by increasing  $V_{CB}$  at  $T_B = T_0$  and at an assigned  $I_E$ , the dissipated power  $P_D$  [W] increases, the junction temperature  $T_j$  increases, and  $V_{BEj}$  decreases almost linearly with  $T_j$ .

Note that (13) can be expressed in terms of the externally-measurable  $V_{BE}$  as follows:

$$V_{BE} - R_B(T_j) \cdot I_B(T_j) - R_E(T_j) \cdot I_E \approx V_{BE}(T_0) - R_B(T_0) \cdot I_B(T_0) - R_E(T_0) \cdot I_E - \phi \cdot (T_j - T_0) \tag{15}$$

By neglecting the  $I_B$  variation with  $T_j$ , and assuming temperature-insensitive parasitic resistances  $R_B$  and  $R_E$  [18], (15) can be rewritten as

$$V_{BE} \approx V_{BE}(T_0) - \phi \cdot (T_j - T_0) \tag{16}$$

that is, the  $V_{BE}-T_j$  characteristic is only shifted upward with respect to the  $V_{BEj}-T_j$  counterpart, while exhibiting the same slope  $\left(\phi = -\left.\frac{\partial V_{BEj}}{\partial T_j}\right|_{I_E} \approx -\left.\frac{\partial V_{BE}}{\partial T_j}\right|_{I_E}\right)$ . If  $I_E$  is selected not too high to neglect high-injection effects ( $B_{HI} \approx 1$ ), then (14) reduces to [1,10,15,16,18,19,31,44,45]

$$\phi = \phi_0 - \eta \cdot \frac{k}{q} \cdot \ln \frac{I_E}{A_E \cdot J_{S0}} \tag{17}$$

### 2.2. Thermal Resistance

As mentioned in Section 1, the static thermal behavior of a semiconductor device is well described by the self-heating thermal resistance  $R_{TH}$  [K/W], which represents an indicator of the *inability* of the component to remove heat from the power dissipation region (simply denoted as *heat source*). By specifically referring to a bipolar transistor,  $R_{TH}$  is defined as

$$R_{TH} = \frac{T_j - T_B}{P_D} = \frac{\Delta T_j}{P_D} \tag{18}$$

where  $\Delta T_j$  is the junction temperature rise above backside and  $P_D$  is the dissipated power, given by

$$P_D = I_B \cdot V_{BE} + I_C \cdot V_{CE} = I_E \cdot V_{BE} + I_C \cdot V_{CB} \tag{19}$$

The thermal resistance depends on (i) device and heat source geometry, (ii) thermal conductivities of the materials crossed by the heat emerging from the source, and (iii) boundary conditions. A transistor with a horizontally- and/or vertically-scaled heat source suffers from a higher  $R_{TH}$  since for the same  $P_D$  the dissipated power *density* is higher, and therefore  $T_j$  is also higher. Similarly, the adoption of materials with low thermal conductivities hinders the heat flow, thus leading to an increase in  $R_{TH}$ .

In addition, it must be considered that the thermal conductivities  $k$  [W/ $\mu\text{mK}$ ] of semiconductors and metals in a transistor decrease with temperature ([46] and references therein), thereby lowering the heat transfer efficiency. The thermally-induced  $k$  degradation introduces a *nonlinearity* in the heat conduction equation, and the resulting effects are referred to as *nonlinear thermal effects*. The device temperature in turn increases for *two distinct physical mechanisms*: (i) the increase in backside temperature  $T_B$  (*nonlinear thermal effect due to backside temperature*) and (ii) the increase in dissipated power  $P_D$  (*nonlinear self-heating effect*). Consequently,  $R_{TH}$  is a monotonically-growing function of both  $T_B$  and

$P_D$ , and should be more properly formulated as  $R_{TH}(T_B, P_D)$ , where the dependence on  $T_B$  and  $P_D$  implicitly comes from the  $k$  reduction with increasing temperature [47].

### 3. Simulation Approach

#### 3.1. Devices under Test

Similar to [46], the analysis was conducted on two NPN HBT technologies.

The InGaP/GaAs NPN HBT is a mesa-isolated device manufactured by Qorvo with four  $2 \times 20.5 \mu\text{m}^2$  emitter fingers (and thus the total emitter area amounts to  $164 \mu\text{m}^2$ ). The GaAs substrate is  $620 \mu\text{m}$  thick and equipped with  $65 \times 65 \mu\text{m}^2$  pads in a ground-signal-ground configuration for bare-die experimental characterization through RF probes. The key features of this device are reported in Table 1. Further technological details are provided in [15].

**Table 1.** Key features of the InGaP/GaAs NPN HBT under test.

Parameter	Value
Common-emitter current gain $\beta_F$ at 300 K and medium current levels	150
Open-emitter breakdown voltage $BV_{CBO}$	27 V
Open-base breakdown voltage $BV_{CEO}$	17 V
Peak cut-off frequency $f_T$ for $V_{CE} = 3$ V	40 GHz
Collector current density $J_C$ at peak $f_T$ for $V_{CE} = 3$ V	$0.2 \text{ mA}/\mu\text{m}^2$
Maximum oscillation frequency $f_{max}$ for $V_{CE} = 3$ V	82 GHz

The Si/SiGe NPN HBT was fabricated by Infineon Technologies AG in the framework of the European Project DOTFIVE. The device has only one base and one collector contact (BEC configuration), and belongs to the latest project technology stage, also denoted as set #3 in [18,44]. The drawn emitter area is equal to  $0.2 \times 2.8 \mu\text{m}^2$ , and the substrate is  $185 \mu\text{m}$  thick. The figures of merit of this device are listed in Table 2.

**Table 2.** Key features of the Si/SiGe NPN HBT under test.

Parameter	Value
Common-emitter current gain $\beta_F$ at 300 K and medium current levels	2200
Open-emitter breakdown voltage $BV_{CBO}$	5.5 V
Open-base breakdown voltage $BV_{CEO}$	1.6 V
Peak cut-off frequency $f_T$ for $V_{CB} = 0.5$ V	240 GHz
Collector current density $J_C$ at peak $f_T$ for $V_{CB} = 0.5$ V	$10 \text{ mA}/\mu\text{m}^2$
Maximum oscillation frequency $f_{max}$ for $V_{CB} = 0.5$ V	380 GHz

#### 3.2. Transistor Model

We chose to resort to an *in-house* analytical model to describe the DC operation of the bipolar transistor, as it is simple, accurate enough, and enables a low-effort parameter extraction procedure. This offers high flexibility throughout the whole investigation. The collector current  $I_C$  in forward active mode is expressed as [15,44,45]

$$I_C = M \cdot I_{CT} = M \cdot \left(1 + \frac{V_{CB}}{V_{AF}}\right) \cdot \frac{1}{B_{HI}} \cdot A_E \cdot J_{S0} \cdot \exp\left[\frac{V_{BEj} + \phi \cdot (T_j - T_0)}{\eta \cdot V_{T0}}\right] \quad (20)$$

where all terms have the same meaning as in Section 2.1, and coefficient  $\phi$  is given by the logarithmic law (10). In this approach, the temperature dependence of  $I_C$  is taken into account with a  $V_{BEj}$  shift, while the reverse saturation current density  $J_{S0}$  and the thermal voltage  $V_{T0} = kT_0/q$  are kept at their  $T_0$  values (e.g., [48]).

As far as the avalanche factor  $M$  is concerned, any model can in principle be adopted. For the InGaP/GaAs HBT under test, we chose the classic Miller formulation given by [49]

$$M = \frac{1}{1 - \left(\frac{V_{CB}}{BV_{CBO}}\right)^{n_{AV}}} \tag{21}$$

where  $BV_{CBO}$  [V] is the open-emitter breakdown voltage and the dimensionless  $n_{AV}$  ( $>0$ ) is a fitting power factor. For the Si/SiGe HBT, we selected the more complex model [50,51]

$$M = 1 + a_{AV} \cdot \frac{V_{CB}/BV_{CBO}}{1 - V_{CB}/BV_{CBO}} \cdot \exp\left[-b_{AV} \cdot \left(\frac{V_{CB}}{BV_{CBO}}\right)^{-c_{AV}}\right] \tag{22}$$

where  $a_{AV}$ ,  $b_{AV}$ , and  $c_{AV}$  (all  $> 0$ ) are dimensionless fitting parameters.

The high-injection (high-current) attenuation term is modeled as [15,44,45,52]

$$B_{HI} = 1 + \left(\frac{I_C}{A_E \cdot J_{HI}}\right)^{n_{HI}} \tag{23}$$

where  $J_{HI}$  [A/cm<sup>2</sup> or A/μm<sup>2</sup>] and  $n_{HI}$  ( $>0$ ) are fitting parameters.

The common-emitter forward current gain  $\beta_F$  is described as [15,18,44,45]

$$\beta_F = \beta_{F0} \cdot \left(1 + \frac{V_{CB}}{V_{AF}}\right) \cdot \frac{1}{B_{HI}} \cdot \exp\left[\frac{\Delta E_{GEB}}{k} \cdot \left(\frac{1}{T_j} - \frac{1}{T_0}\right)\right] \tag{24}$$

where  $\beta_{F0}$  is the gain at  $T_0$ , at medium current levels (i.e., before the high-injection-induced fall-off) and in the absence of Early effect, while  $\Delta E_{GEB} = E_{GE} - E_{GB}$  [eV] is the difference between the bandgaps of emitter and base, which is positive in HBTs and entails a negative temperature coefficient of  $\beta_F$ , and negative in BJTs (due to the band-gap narrowing in the heavily doped emitter), where it leads to a positive temperature coefficient.

The base current  $I_B$  is given by

$$I_B = I_{BT} - I_{AV} \tag{25}$$

where  $I_{BT}$  [A] is the current of holes injected into the emitter and  $I_{AV}$  is the avalanche-induced current of holes exiting the base terminal (or equivalently of electrons entering the collector terminal). Considering that

$$I_{BT} = \frac{I_{CT}}{\beta_F} \tag{26}$$

and that  $I_{AV}$  can also be expressed as

$$I_{AV} = I_C - I_{CT} = (M - 1) \cdot I_{CT} \tag{27}$$

then (25) becomes [15,42,45]

$$I_B = \frac{I_{CT}}{\beta_F} - (M - 1) \cdot I_{CT} = I_{CT} \cdot \left(\frac{1 + \beta_F}{\beta_F} - M\right) = I_C \cdot \left(\frac{1}{\alpha_F \cdot M} - 1\right) \tag{28}$$

$\alpha_F$  being the common-base forward current gain. The emitter current  $I_E$  is obviously given by  $I_C + I_B$ .

The static power-temperature feedback (i.e., the evaluation of  $T_j$  from  $P_D$ ) including nonlinear thermal effects is accounted for according to the conclusions reached in [46], which can be summarized as follows. Hereafter,  $R_{TH00}$  will conventionally denote the

thermal resistance of the bipolar transistor at  $T_B = T_0$  and very low  $P_D$  (*ideally* for  $P_D \rightarrow 0$  W, i.e., in the absence of the nonlinear self-heating effect), that is,

$$R_{TH00} = R_{TH}(T_B = T_0, P_D \rightarrow 0) \quad (29)$$

In simple terms,  $R_{TH00}$  represents the thermal resistance of the transistor if the thermal conductivities of all materials are equal to their  $k(T_0)$  value. The low-power thermal resistance  $R_{THB0}$  at an arbitrary  $T_B$  in the range 250 to 450 K (*nonlinear thermal effect due to the backside temperature*) can be calculated as [22,26,47,53]

$$R_{THB0} = R_{TH00} \cdot \left( \frac{T_B}{T_0} \right)^\alpha \quad (30)$$

where  $\alpha$  ( $>0$ ) is a dimensionless fitting parameter. The further thermal resistance growth due to the increase in  $P_D$  (*nonlinear self-heating effect*) can be accounted for by invoking the Kirchhoff transformation as [5,22,26,47,53]

$$R_{TH}(T_B, P_D) = \frac{T_B}{P_D} \cdot \left\{ \left[ 1 - (\alpha - 1) \cdot \frac{R_{THB0} \cdot P_D}{T_B} \right]^{\frac{-1}{\alpha-1}} - 1 \right\} \quad (31)$$

where  $\alpha$  is the same parameter applied in (30). Using (30) in (31), the following  $R_{TH}$  expression is obtained:

$$R_{TH}(T_B, P_D) = \frac{T_B}{P_D} \cdot \left\{ \left[ 1 - (\alpha - 1) \cdot \frac{R_{TH00} \cdot P_D}{T_B \cdot \left( \frac{T_0}{T_B} \right)^\alpha} \right]^{\frac{-1}{\alpha-1}} - 1 \right\} \quad (32)$$

In [46],  $R_{TH}$  was determined for the InGaP/GaAs HBT and the Si/SiGe HBT under test in reasonably wide ranges of  $T_B$  and  $P_D$  by extremely detailed nonlinear COMSOL [54] simulations, and it was observed that (32) allows obtaining a good agreement with COMSOL data if a “brute-force 2-D search” of parameters  $R_{TH00}$  and  $\alpha$  is performed, as suggested in [26]. Conveniently, it was found that the optimized  $R_{TH00}$  is very close to that computed by COMSOL, regardless of the HBT technology.

### 3.3. Circuit-Based Electrothermal Simulation

The model detailed in Section 3.2 was implemented in the popular PSPICE circuit simulator [55] as a *subcircuit*, where the standard bipolar transistor instance is used as a *core* component at temperature  $T_0$ . Besides the collector, emitter, and base terminals, the subcircuit is equipped with an additional (input) thermal node and an additional (output) power node. The thermal node is fed with the temperature rise  $\Delta T_j = T_j - T_B$ , while the power node provides the dissipated power  $P_D$ , internally computed according to (19). Apart from the standard transistor, the subcircuit is enhanced with linear/nonlinear controlled voltage/current sources to enable the variation of the temperature-sensitive parameters during the simulation run, as well as to account for avalanche, Early, and high-injection effects. Further details are given in [15].

Equation (32) is in turn implemented as follows (solution #1 in [46]). First,  $R_{THB0}$  is evaluated in the pre-simulation stage from (30) at the assigned  $T_B$ , and the dissipated power  $P_D$  (a current in PSPICE) is forced to flow into  $R_{THB0}$  (an electrical resistance). The temperature rise (a voltage drop) given by  $R_{THB0} \cdot P_D$  is provided as input to a behavioral block (a nonlinear voltage-controlled voltage source) that calculates  $\Delta T_j$  as

$$\Delta T_j = T_B \cdot \left[ 1 - (\alpha - 1) \cdot \frac{R_{THB0} \cdot P_D}{T_B} \right]^{\frac{-1}{\alpha-1}} - T_B \quad (33)$$

which is then forced to the thermal node of the subcircuit;  $T_j = T_B + \Delta T_j$  influences the collector current  $I_C$  (20) and the common-emitter current gain  $\beta_F$  (24).

### 3.4. Validation Methodology

The parameters of the transistor model described in Section 3.2 were tuned to achieve a good agreement between the DC ET characteristics of the devices under test simulated with PSPICE and experimental data. Here the calibration procedure is omitted for the sake of brevity. In (30) and (32),  $R_{TH00} = 460$  K/W and  $\alpha = 0.95$  for the InGaP/GaAs HBT, and  $R_{TH00} = 6855.8$  K/W and  $\alpha = 1.333$  for the Si/SiGe HBT.

Then, DC ET simulations of the devices are performed in PSPICE to emulate the experimental current/voltage data needed for the application of the thermometer-based techniques (Section 4). The extracted  $R_{TH}$  results are then compared to the target formulation (32) embedded in the transistor model. This is equivalent to feeding the techniques with ideal (noiseless) measurements; as a consequence, any disagreement between the extracted data and (32) is only ascribable to the nature of the adopted extraction technique. The approach of using simulation data (also referred to as synthetic data) based on a known target model has been already applied in many previous works dealing with bipolar transistors [20,22,31,41,56–58].

It is worth noting that we are currently conducting a similar analysis also for other HBT technologies by means of Keysight ADS [59] simulations of advanced compact transistor models such as AgilentHBT [60] and HICUM [61] equipped with an  $R_{TH}$  given by the target (32). Until now, the findings are in line with those shown and discussed in Section 4.

## 4. Analysis of Thermometer-Based Experimental $R_{TH}$ Extraction Techniques

In this section, the thermometer-based  $R_{TH}$  extraction techniques are discussed in chronological order by using a unified and comprehensible nomenclature. First, the analytical theory behind them is explained in detail; then, the techniques are applied to synthetic current/voltage data obtained with DC ET PSPICE simulations of the transistor models corresponding to the devices under test introduced in Section 3.1; finally, the extracted data are compared to the target (32).

The pioneering method of Waldrop et al. [23], which exploits  $\beta_F$  as a TSEP, is excluded from the review, since it is based on a complex and time-consuming procedure difficult to implement in an extraction code, as correctly noticed in [40,41]. Consequently, all the techniques presented in the following make use of  $V_{BE}$  as TSEP. All of them must be applied to a transistor operated in forward active mode at a backside temperature  $T_B \geq T_0$ .

### 4.1. Dawson et al. [24]

In the historically-important paper of Dawson et al. [24], the  $R_{TH}$  extraction is made in a two-fold way, namely, using either  $\beta_F$  or  $V_{BE}$  as TSEPs. Hereafter only the approach based on  $V_{BE}$  is considered.

As a first step, the authors calibrate the thermometer on a device with a ground-signal-ground (GSG, with grounded emitter) configuration as follows.  $V_{BE}$  is measured as a function of  $T_B$  by keeping constant  $I_E$  and  $V_{CE}$ . To ensure a constant  $I_E$ ,  $I_B$  is tuned at each  $T_B$ , which is not a simple task. Dawson et al. observe that  $V_{BE}$  shows a nearly linear decrease with  $T_B$  and determine the absolute value  $\phi'$  of the slope of the straight line described by

$$V_{BE} = V_{BE}(T_B = T_0) - \phi' \cdot (T_B - T_0) \quad (34)$$

allowing the best fit at low/medium  $T_B$  values. Subsequently, they assume negligible self-heating, i.e.,  $T_j \approx T_B$ ,  $\phi' \approx \phi$ , so that (34) can be approximated with (16).

By exploiting (18), (16) becomes

$$V_{BE} = V_{BE}(T_0) - \phi \cdot (T_B + R_{TH} \cdot P_D - T_0) = V_{BE}(T_0) - \phi \cdot (T_B - T_0) - \phi \cdot R_{TH} \cdot P_D \quad (35)$$

The  $V_{BE}-T_B$  characteristics are then measured at different  $V_{CE}$  values (low enough to avoid avalanche) at the same  $I_E$ . This allows plotting the  $I_E$ -constant  $V_{BE}-V_{CE}$  curves at each  $T_B$ , and from simple elaboration also the corresponding  $V_{BE}-P_D$  curves, which exhibit a linearly decreasing behavior as well. By considering the  $T_B = T_0$  case, (35) reduces to

$$V_{BE} = V_{BE}(T_0) - \phi \cdot R_{TH} \cdot P_D \quad (36)$$

Dawson et al. extract the (negative) slope

$$\nu = \frac{dV_{BE}}{dP_D} = -\phi \cdot R_{TH} \quad (37)$$

whence  $R_{TH}$  is simply calculated as

$$R_{TH} = -\frac{\nu}{\phi} = \frac{|\nu|}{\phi} \quad (38)$$

Apart from the practical problem of continuously tuning  $I_B$  to hold  $I_E$  constant (as pointed out in [25]), which can be solved by fabricating an identical device with accessible emitter pad, this technique is based on a simple mathematical theory and seems to be reliable. However, there are various mechanisms that potentially affect the accuracy of the  $R_{TH}$  extraction (and can in principle also jeopardize improved variants of the technique). Such mechanisms are explained in detail in the following subsections.

#### 4.1.1. Significant Self-Heating in the Thermometer Calibration

In (38), Dawson et al. do *not* use the coefficient  $\phi$  describing the slope of the  $V_{BEj}-T_j$  behavior, but rather the absolute value  $\phi'$  of the slope of the straight line matching with the experimental  $I_E$ - and  $V_{CE}$ -constant  $V_{BE}-T_B$  characteristic, that is, they actually evaluate  $R_{TH}$  as

$$R_{TH} = \frac{|\nu|}{\phi'} \quad (39)$$

The approximation  $\phi' \approx \phi$  could in principle be inaccurate, since  $\phi$  depends on  $I_E$  and thus the  $I_E$  used in the first measurement (thermometer calibration) must be *the same* applied in the second measurement (leading to the  $I_E$ -constant  $V_{BE}-P_D$  characteristic at  $T_B = T_0$ ), where an appreciable self-heating should be ensured; consequently, the  $I_E$  used in the first measurement cannot be very low, and this unavoidably leads to non-negligible self-heating even for the smallest  $V_{CE}$  driving the transistor into forward active mode. This mechanism can be analytically described as follows [18]. As explained in Section 2.1, for an assigned  $I_E$ , by neglecting the variation of the voltage drops over the parasitic base and emitter resistances due to self-heating, if  $T_B$  is swept,  $V_{BE}$  linearly decreases with  $T_j$  according to (16), where the absolute value  $\phi$  of the slope only depends on  $I_E$  for HBTs marginally impacted by the Early effect. Let us start from (35), derived by (16) and (18), and let us use (19) for the dissipated power  $P_D$ . It is obtained that

$$\begin{aligned} V_{BE} &= V_{BE}(T_0) - \phi \cdot (T_B - T_0) - \phi \cdot R_{TH} \cdot (I_E \cdot V_{BE} + I_C \cdot V_{CB}) \\ &\approx V_{BE}(T_0) - \phi \cdot (T_B - T_0) - \phi \cdot R_{TH} \cdot I_E \cdot (V_{BE} + V_{CB}) \end{aligned} \quad (40)$$

whence

$$V_{BE} = \frac{V_{BE}(T_0) - \phi \cdot R_{TH} \cdot I_E \cdot V_{CB}}{1 + \phi \cdot R_{TH} \cdot I_E} - \frac{\phi}{1 + \phi \cdot R_{TH} \cdot I_E} \cdot (T_B - T_0) = V_{BE}(T_B = T_0) - \phi' \cdot (T_B - T_0) \quad (41)$$

It should be noted that (i) in the common-emitter  $I_E$ -constant  $V_{BE}-T_B$  measurement performed by Dawson et al.,  $V_{CB}$  is almost unchanged (in other techniques, this measurement is executed under common-base conditions with constant  $V_{CB}$ ); (ii)  $T_B = T_0$ , in the presence of self-heating, corresponds to  $T_j > T_0$ ; consequently,  $V_{BE}(T_B = T_0)$  is lower than  $V_{BE}(T_0) = V_{BE}(T_j = T_0)$ ; (iii) as the most important finding inferred from (41), coefficient  $\phi'$  extracted by Dawson et al. is lower than the  $\phi$  that should be actually adopted in (38), and this could in principle lead to an overestimation of  $R_{TH}$ . However, it must be remarked that this analysis only focuses on *linear* thermal effects; the influence of *nonlinear* thermal effects is discussed in Section 4.1.4.

#### 4.1.2. Significant Temperature-Induced Variation of the Voltage Drop over the Base Resistance

If a high  $I_E$  is selected for the extraction, the variation in the base current  $I_B$  with temperature cannot be disregarded any longer (especially if  $R_B$  is high), and (16) no longer holds; instead, for temperature-insensitive parasitic resistances, (15) reduces to

$$V_{BE} - R_B \cdot I_B(T_j) = V_{BE}(T_0) - R_B \cdot I_B(T_0) - \phi \cdot (T_j - T_0) \quad (42)$$

By applying (18)

$$V_{BE} = V_{BE}(T_0) + R_B \cdot [I_B(T_j) - I_B(T_0)] - \phi \cdot R_{TH} P_D - \phi \cdot (T_B - T_0) \quad (43)$$

and then (19)

$$V_{BE} = V_{BE}(T_0) + R_B \cdot [I_B(T_j) - I_B(T_0)] - \phi \cdot R_{TH} \cdot I_E \cdot (V_{BE} + V_{CB}) - \phi \cdot (T_B - T_0) \quad (44)$$

it is obtained that

$$V_{BE} = \frac{V_{BE}(T_0) - \phi \cdot R_{TH} \cdot I_E \cdot V_{CB}}{1 + \phi \cdot R_{TH} \cdot I_E} + \frac{R_B \cdot [I_B(T_j) - I_B(T_0)]}{1 + \phi \cdot R_{TH} \cdot I_E} - \frac{\phi}{1 + \phi \cdot R_{TH} \cdot I_E} \cdot (T_B - T_0) \quad (45)$$

By increasing  $T_B$  for a constant  $I_E$ ,  $I_C(T_j)$  decreases due to the negative temperature coefficient of  $\beta_F$ , and thus  $I_B(T_j)$  increases. When such effect is not negligible, the actual absolute value  $\phi'$  of the slope of the  $V_{BE}-T_B$  characteristic is even lower than  $\frac{\phi}{1 + \phi \cdot R_{TH} \cdot I_E}$ , and this could cause an overestimation of  $R_{TH}$  more marked than that dictated only by the linear self-heating [18].

On the other hand, let us focus on the second step aiming at the  $R_{TH}$  assessment, i.e., the extraction of the slope  $\nu$  of the  $I_E$ -constant  $V_{BE}-P_D$  curve at  $T_B = T_0$ . In this case, (43) becomes

$$V_{BE} \approx V_{BE}(T_0) + R_B \cdot [I_B(T_j) - I_B(T_0)] - \phi \cdot R_{TH} P_D \quad (46)$$

By increasing  $P_D$  at a constant  $I_E$ ,  $I_B(T_j)$  grows, and then the absolute value of the slope  $|\nu|$  is lower than  $\phi \cdot R_{TH}$ , which could lead to an underestimation of  $R_{TH}$  [18]. In conclusion, applying a high  $I_E$  gives rise to two counteracting effects: a further reduction of the extracted  $\phi'$  with respect to  $\phi$  that could lead to an overestimation in  $R_{TH}$ ; a reduction of the slope  $|\nu|$  with respect to  $\phi \cdot R_{TH}$  that could yield an underestimation in  $R_{TH}$ . In general, it is difficult to predict which effect dominates.

#### 4.1.3. Significant Early Effect

If significant, the Early effect can be misinterpreted by the extraction technique as an additional overheating, thus leading to an overestimation of  $R_{TH}$  [19,31,56]. This can be analytically explained as follows. Let us neglect that  $\phi$  is sensitive to the Early effect and increases with  $V_{CB}$ . Under biasing conditions at which avalanche and high-injection effects can be neglected, (20) reduces to

$$\begin{aligned}
 I_C &= \left(1 + \frac{V_{CB}}{V_{AF}}\right) \cdot A_E \cdot J_{S0} \cdot \exp\left[\frac{V_{BEj} + \phi \cdot (T_j - T_0)}{\eta \cdot V_{T0}}\right] = \left(1 + \frac{V_{CB}}{V_{AF}}\right) \cdot A_E \cdot J_{S0} \cdot \exp\left[\frac{V_{BE} - R_{EB} \cdot I_B - R_E \cdot I_E + \phi \cdot (T_j - T_0)}{\eta \cdot V_{T0}}\right] \\
 &\approx \left(1 + \frac{V_{CB}}{V_{AF}}\right) \cdot A_E \cdot J_{S0} \cdot \exp\left[\frac{V_{BE} - R_{EB} \cdot I_C + \phi \cdot (T_j - T_0)}{\eta \cdot V_{T0}}\right]
 \end{aligned} \tag{47}$$

where  $R_{EB} = \frac{R_B + R_E}{\beta_F} + R_E$ . Assuming  $T_B = T_0$  and absence of self-heating, then  $T_j = T_0$  and (47) becomes

$$I_C = \left(1 + \frac{V_{CB}}{V_{AF}}\right) \cdot A_E \cdot J_{S0} \cdot \exp\left[\frac{V_{BE}(T_0) - R_{EB} \cdot I_C}{\eta \cdot V_{T0}}\right] \tag{48}$$

from which  $V_{BE}(T_0)$  can be determined as

$$V_{BE}(T_0) = R_{EB} \cdot I_E + \eta \cdot V_{T0} \cdot \ln \frac{I_E}{\left(1 + \frac{V_{CB}}{V_{AF}}\right) \cdot A_E \cdot J_{S0}} \tag{49}$$

where use has been made of the approximation  $I_C \approx I_E$ . By substituting (49) into (16),

$$V_{BE} = R_{EB} \cdot I_E + \eta \cdot V_{T0} \cdot \ln \frac{I_E}{\left(1 + \frac{V_{CB}}{V_{AF}}\right) \cdot A_E \cdot J_{S0}} - \phi \cdot (T_j - T_0) \tag{50}$$

and using (18)

$$V_{BE} = R_{EB} \cdot I_E + \eta \cdot V_{T0} \cdot \ln \frac{I_E}{\left(1 + \frac{V_{CB}}{V_{AF}}\right) \cdot A_E \cdot J_{S0}} - \phi \cdot R_{TH} \cdot P_D - \phi \cdot (T_B - T_0) \tag{51}$$

which at  $T_B = T_0$  becomes

$$V_{BE} = R_{EB} \cdot I_E + \eta \cdot V_{T0} \cdot \ln \frac{I_E}{\left(1 + \frac{V_{CB}}{V_{AF}}\right) \cdot A_E \cdot J_{S0}} - \phi \cdot R_{TH} \cdot P_D \tag{52}$$

It can be inferred that, due to the Early effect, the absolute value  $|\nu|$  of the slope of the  $I_E$ -constant  $V_{BE}-P_D$  curve at  $T_B = T_0$  is higher than that due to self-heating only, as  $V_{CB}$  increases and leads to a reduction in  $V_{BE}(T_0)$ ; this is misinterpreted by the techniques as an additional self-heating, so that  $R_{TH}$  could be overestimated.

It will be seen that the Early effect has a perceptible influence only on the extraction results corresponding to the Si/SiGe HBT under test, the  $V_{AF}$  of which is high, but lower than that of the InGaP/GaAs transistor.

#### 4.1.4. Significant Nonlinear Thermal Effects

For the sake of simplicity, let us disregard the mechanisms explored in Sections 4.1.2 and 4.1.3. As mentioned in Section 2.2, nonlinear thermal effects make the thermal resistance a monotonically-increasing function of  $T_B$  and  $P_D$ ; as a consequence, (41) should be more correctly formulated as

$$V_{BE} = \frac{V_{BE}(T_0) - \phi \cdot R_{TH}(T_B, P_D) \cdot I_E \cdot V_{CB}}{1 + \phi \cdot R_{TH}(T_B, P_D) \cdot I_E} - \frac{\phi}{1 + \phi \cdot R_{TH}(T_B, P_D) \cdot I_E} \cdot (T_B - T_0) \tag{53}$$

In the first measurement,  $P_D$  is almost constant, and  $R_{TH}(T_B, P_D)$  increases due to the  $T_B$  sweep. By approximating the  $V_{BE}-T_B$  data with a straight line, it is found that the absolute value  $\phi'$  of the slope of this line is *higher* than  $\frac{\phi}{1 + \phi \cdot R_{TH00} \cdot I_E}$ , which means that the error due to the presence of the nonlinear thermal effect associated to the  $T_B$  increase gives rise to an unquantifiable compensation of the error associated to the presence of the *linear* self-heating.

In the second measurement,  $T_B = T_0$  and (36) becomes

$$V_{BE} = V_{BE}(T_0) - \phi \cdot R_{TH}(T_0, P_D) \cdot P_D \quad (54)$$

Here,  $V_{BE}$  reduces more than linearly with  $P_D$ , as  $R_{TH}(T_0, P_D)$  increases with  $P_D$  (nonlinear self-heating effect), which leads to an extracted  $|\nu|$  higher than that dictated by the linear self-heating; this causes an overestimation of  $R_{TH}$  with respect to  $R_{TH00}$ , which is expected to be exacerbated as the  $P_D$  range wherein the extraction is carried out increases.

As a rule of thumb, it would be better to apply the lowest  $I_E$  giving rise to perceptible self-heating and a rather narrow  $P_D$  range in order to prevent a significant nonlinear self-heating effect during the second measurement. Unfortunately, the self-heating and nonlinear thermal effect due to the  $T_B$  increase during the thermometer calibration cannot be fully disregarded: the extracted  $\phi'$  can be lower than  $\phi$  if the first effect prevails or higher than  $\phi$  if the second dominates.

For the InGaP/GaAs HBT,  $I_E = 10$  mA and  $V_{CE} = 2$  V were chosen with the aim to keep the device in forward active mode, minimize the self-heating and the nonlinear thermal effect due to  $T_B$  in the first measurement, and (with reference solely to  $I_E = 10$  mA) ensure a perceptible self-heating during the second measurement. The extracted  $\phi'$  is 1.175 mV/K (higher than  $\phi = 1.141$  mV/K, as the nonlinear thermal effect due to  $T_B$  prevails over the linear self-heating), while the extracted  $R_{TH}$  is 468.1 K/W by superiorly limiting the  $P_D$  range to 0.03 W, with an error of 1.76% with respect to  $R_{TH00} = 460$  K/W induced by the nonlinear self-heating effect in the second measurement.

For the Si/SiGe HBT,  $I_E = 1$  mA and  $V_{CE} = 1$  V were selected. The extracted  $\phi'$  is 0.856 mV/K (higher than  $\phi = 0.829$  mV/K for the same reason). The extracted  $R_{TH}$  is 7196.7 K/W by superiorly limiting the  $P_D$  range to 1.5 mW, with an error equal to 5% with respect to  $R_{TH00} = 6855.8$  K/W due to the Early and the nonlinear self-heating effect in the second measurement.

In conclusion, in both cases  $R_{TH} > R_{TH00}$ , since the inaccuracy in the second step dominates over the error leading to  $\phi' > \phi$  in the first step, which paradoxically plays a beneficial compensation role.

#### 4.2. Bovolon et al. [25]

Dawson et al. [24] observe that only two backside temperatures  $T_B$  and  $T_B + \Delta T_B$  and two power dissipation levels  $P_D$  and  $P_D + \Delta P_D$  are in principle needed to determine  $R_{TH}$  ("differential" variant of the approach). Coefficient  $\phi$  can be indeed calculated as

$$\phi = \frac{V_{BE}(T_B, P_D) - V_{BE}(T_B + \Delta T_B, P_D)}{\Delta T_B} \quad (55)$$

and the (negative) slope  $\nu$  as

$$\nu = \frac{V_{BE}(T_B, P_D + \Delta P_D) - V_{BE}(T_B, P_D)}{\Delta P_D} \quad (56)$$

so that (38) becomes

$$R_{TH} = \frac{|\nu|}{\phi} = \frac{\frac{V_{BE}(T_B, P_D) - V_{BE}(T_B, P_D + \Delta P_D)}{\Delta P_D}}{\frac{V_{BE}(T_B, P_D) - V_{BE}(T_B + \Delta T_B, P_D)}{\Delta T_B}} \quad (57)$$

The technique proposed by Bovolon et al. [25] can be considered as an extension of the "differential" variant of the approach by Dawson et al., as it allows determining the influence of nonlinear thermal effects (i.e., the  $T_B$  and  $P_D$  dependences of  $R_{TH}$ ). In the

assumption of validity of (16), Bovolon et al. observe that the linear  $V_{BE}$  decrease with  $T_j$  also takes place locally, i.e., around a certain junction temperature  $T_j^*$ :

$$V_{BE} = V_{BE}(T_j^*) - \phi \cdot (T_j - T_j^*) \quad (58)$$

By exploiting (18) and accounting for nonlinear thermal effects, (58) becomes

$$V_{BE}(T_B, P_D) = V_{BE}(T_j^*) - \phi \cdot [T_B + R_{TH}(T_B, P_D) \cdot P_D - T_j^*] \quad (59)$$

If (59) is applied to another backside temperature  $T_B + \Delta T_B$  at the same dissipated power  $P_D$ ,

$$V_{BE}(T_B + \Delta T_B, P_D) = V_{BE}(T_j^*) - \phi \cdot [T_B + \Delta T_B + R_{TH}(T_B + \Delta T_B, P_D) \cdot P_D - T_j^*] \quad (60)$$

Let us subtract (60) from (59) by assuming  $\Delta T_B$  sufficiently low to neglect the related  $R_{TH}$  variation; this leads to

$$V_{BE}(T_B, P_D) - V_{BE}(T_B + \Delta T_B, P_D) \approx \phi \cdot \Delta T_B \quad (61)$$

so that

$$\phi \approx \frac{V_{BE}(T_B, P_D) - V_{BE}(T_B + \Delta T_B, P_D)}{\Delta T_B} \quad (62)$$

If (59) is applied to another dissipated power  $P_D + \Delta P_D$ ,

$$V_{BE}(T_B, P_D + \Delta P_D) = V_{BE}(T_j^*) - \phi \cdot [T_B + R_{TH}(T_B, P_D + \Delta P_D) \cdot (P_D + \Delta P_D) - T_j^*] \quad (63)$$

Let us subtract (63) from (59) by assuming that  $\Delta P_D$  is sufficiently small to disregard the related  $R_{TH}$  variation and the  $\phi$  dependence on  $I_E$ ; it is obtained that

$$V_{BE}(T_B, P_D) - V_{BE}(T_B, P_D + \Delta P_D) \approx \phi \cdot R_{TH}(T_B, P_D) \cdot \Delta P_D \quad (64)$$

Finally, by combining (62) and (64),

$$R_{TH}(T_B, P_D) = \frac{\frac{V_{BE}(T_B, P_D) - V_{BE}(T_B, P_D + \Delta P_D)}{\Delta P_D}}{\frac{V_{BE}(T_B, P_D) - V_{BE}(T_B + \Delta T_B, P_D)}{\Delta T_B}} \quad (65)$$

By repeating the extraction for different values of backside temperature  $T_B$  and dissipated power  $P_D$ ,  $R_{TH}$  can be determined as a function of  $T_B$  and  $P_D$  without imposing analytical assumptions on both dependences.

For each  $T_B$ , the technique requires the measurement of  $V_{BE}$  and  $I_C$  by sweeping  $V_{CE}$  under  $I_B$ -constant conditions at  $T_B$  and  $T_B + \Delta T_B$ . The evaluation of  $R_{TH}(T_B, P_D)$  at the given  $T_B$  is carried out as follows. Once a dissipated power  $P_D$  is chosen, two points with close dissipated powers  $P_D$  and  $P_D + \Delta P_D$  are selected on the  $V_{BE}$ - $V_{CE}$  curve corresponding to  $T_B$ , and the related  $V_{BE}(T_B, P_D)$  and  $V_{BE}(T_B, P_D + \Delta P_D)$  values are used for the calculation of the numerator of (65). Then, the point with dissipated power  $P_D$  has to be also identified on the  $V_{BE}$ - $V_{CE}$  curve corresponding to  $T_B + \Delta T_B$ , and the associated  $V_{BE}(T_B + \Delta T_B, P_D)$  allows the calculation of the denominator of (65). This procedure is repeated for other  $P_D$  values. Then the whole process is applied to another  $T_B$ .

Due to its differential nature ( $R_{TH}$  is determined by two differences between  $V_{BE}$  values measured in *two* points only), this technique is expected to suffer from inaccuracy induced by the following reasons: (i)  $\Delta T_B$  and  $\Delta P_D$  should be chosen sufficiently small to ensure (61) and (64), respectively. However, if  $\Delta T_B$  and  $\Delta P_D$  are too small, the error associated to noisy data is emphasized when calculating  $R_{TH}$  with (65); (ii) the collector currents corresponding to  $P_D$  and  $P_D + \Delta P_D$  should be quite close to safely neglect the  $\phi$  dependence on  $I_E$ ; (iii) since for assigned  $P_D$  and  $\Delta P_D$  values the measurement will not

exactly provide  $V_{BE}(T_B, P_D + \Delta P_D)$  on the first characteristic and  $V_{BE}(T_B + \Delta T_B, P_D)$  on the second, an interpolation between adjacent points might be needed.

For the InGaP/GaAs HBT, the extraction was performed by applying  $I_B = 0.7 \text{ mA}$ ,  $\Delta P_D = 10 \text{ mW}$ ,  $\Delta T_B = 10 \text{ K}$ . For the Si/SiGe HBT, it was carried out by applying  $I_B = 2.5 \text{ }\mu\text{A}$ ,  $\Delta P_D = 0.1 \text{ mW}$ ,  $\Delta T_B = 10 \text{ K}$ . Unfortunately, in the latter case, the low  $BV_{CEO}$  value ( $=1.6 \text{ V}$ ) leads to a quite narrow  $P_D$  range where the avalanche multiplication is negligible and thus the technique can be adopted. Figure 1 shows the comparison between the  $R_{TH}$  data extracted from DC ET simulations with the target ones evaluated from (32) for both technologies. It can be inferred that the technique of Bovolon et al. roughly predicts the increase in  $R_{THB0}$  with  $T_B$  but fails to describe the  $R_{TH}$  increase with  $P_D$  at a given  $T_B$  (nonlinear self-heating effect) due to the issues mentioned earlier.

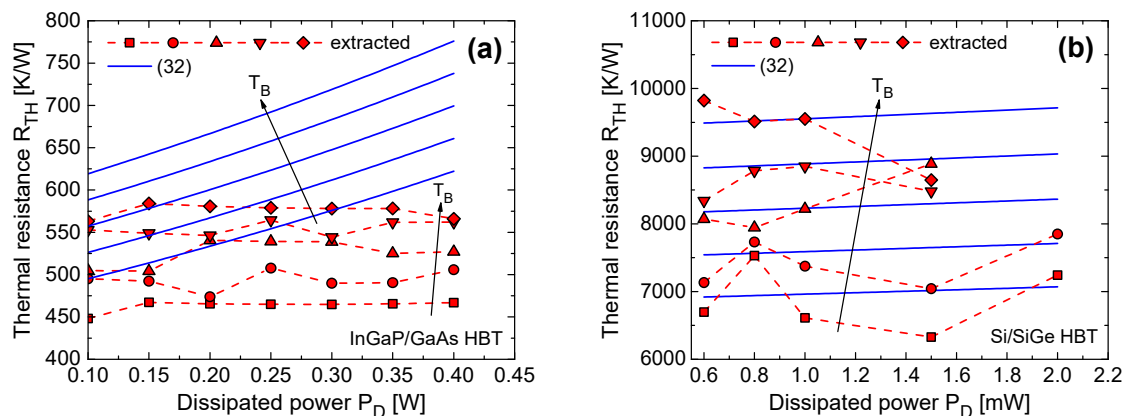


**Figure 1.**  $R_{TH}$  vs.  $P_D$  at various  $T_B$  spanning the range 300 to 380 K with a 20 K step; data extracted with the technique of Bovolon et al. (dashed red lines with symbols) are compared to the target data obtained from (32) (solid blue). (a) InGaP/GaAs HBT; (b) Si/SiGe HBT.

#### 4.3. Yeats [26]

The technique conceived by Yeats [26] can also be reviewed as an improved version of that presented by Dawson et al. [24] in that it allows accounting for both nonlinear thermal effects. Electrical common-base measurements are performed on a transistor equipped with a directly-accessible emitted pad. First, some  $I_E$ -constant  $V_{BE}-V_{CE}$  ( $V_{CE}$  being given by the sum of the forced  $V_{CB}$  and the measured  $V_{BE}$ ) characteristics are measured at various backside temperatures  $T_B$ . Through a quadratic polynomial with  $I_E$ -dependent coefficients, the  $V_{BE}$  values corresponding to  $V_{CE} = 0 \text{ V}$  ( $P_D = 0 \text{ W}$  and thus  $T_j = T_B$ ) are extrapolated, so that the  $V_{BE}-T_j$  thermometer is defined at the assigned  $I_E$ , described by means of another quadratic polynomial with  $I_E$ -dependent coefficients, and then inverted into  $T_j-V_{BE}$ . Hence, any  $V_{BE}$  is associated to the corresponding  $T_j$  value, and the experimental  $I_E$ -constant  $T_j-P_D$  curves at various  $T_B$  are straightforwardly determined. Consequently, the experimental  $R_{TH}(T_B, P_D)$  against  $P_D$  is known for each  $T_B$  from (18).

It is worth noting that this technique *directly* uses the thermometer to evaluate  $R_{TH}$ , differently from other methods that are also based on the differential calculation  $\Delta V_{BE}/\Delta P_D$  [25] or the more robust extraction of the slope  $\nu$  of the  $V_{BE}-P_D$  curve [24,27,29] (or equivalently the extraction of the slope  $\gamma$  of the  $V_{BE}-V_{CB}$  curve [18,31]) under  $I_E$ -constant conditions.

This technique is often applied to GaAs-based HBTs, especially for  $T_j$  estimates used in reliability.

For the InGaP/GaAs and the Si/SiGe HBTs,  $I_E = 20 \text{ mA}$  and  $2 \text{ mA}$  were applied, respectively. Results are shown in Figure 2, where again the extracted data are compared to the target formulation (32). As can be seen, for the InGaP/GaAs HBT, the agreement is excellent. A slight  $R_{TH}$  overestimation is instead obtained for the Si/SiGe HBT while the increase induced by the nonlinear self-heating effect is well described. Such overestimation can be explained as follows. The temperature  $T_j$  is predicted with a very small

overestimation; however, subtracting  $T_B$  and dividing by the small  $P_D$  dissipated in this scaled transistor to calculate  $R_{TH} = \Delta T_j / P_D$  magnifies the error.

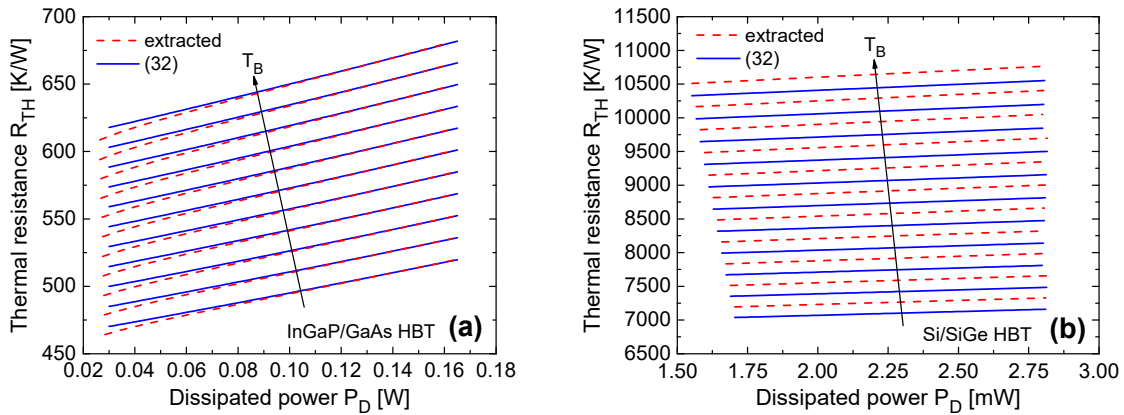


**Figure 2.**  $R_{TH}$  vs.  $P_D$  at various  $T_B$  spanning the range 300 to 400 K with a 10 K step; data extracted with the technique of Yeats (dashed red lines) are compared to the target data obtained from (32) (solid blue). (a) InGaP/GaAs HBT; (b) Si/SiGe HBT.

Although this technique works fairly well on synthetic data, it must be observed that it directly uses the thermometer to determine  $R_{TH}$ , and therefore it is very sensitive to the  $V_{BE}$  values, which can be noisy since are difficult to measure with a high degree of accuracy.

#### 4.4. Pfost et al. [28]

Pfost et al. [28] perform measurements on a transistor in a GSG configuration. They first measure  $V_{CE}$ -constant  $I_C$ - $V_{BE}$  characteristics at various  $T_B$  values, and then derive by interpolation the  $V_{BE}$ - $T_B$  curves at various  $I_C$  values. The  $V_{CE}$  is chosen sufficiently low to safely neglect the avalanche effect, while the Early effect was assumed negligible. The authors then calibrate the thermometer by extracting the absolute value  $\phi'$  of the slope of the straight line ensuring the best fit with the  $V_{BE}$ - $T_B$  curves, and observe that this coefficient depends on the technology, is almost insensitive to the transistor layout, and decreases with  $I_C$ . Then they assume that there is negligible self-heating and thus  $\phi' \approx \phi$ .

Subsequently, Pfost et al. consider that in the absence of avalanche, Early, and high-injection effects, the  $I_C$  formulation (20) reduces to

$$I_C = A_E \cdot J_{S0} \cdot \exp \left[ \frac{V_{BE} - R_{EB} \cdot I_C + \phi \cdot (T_j - T_0)}{\eta \cdot V_{T0}} \right] \quad (66)$$

At low  $V_{BE}$  (low  $I_C$ ), self-heating and resistive effects can be neglected, and (66) turns into

$$I_C \approx A_E \cdot J_{S0} \cdot \exp \left( \frac{V_{BE}}{\eta \cdot V_{T0}} \right) \quad (67)$$

Parameters  $J_{S0}$  and  $\eta$  can be extracted by comparing the experimental  $V_{CE}$ -constant  $I_C$ - $V_{BE}$  curve at  $T_B = T_0$  with (67) at low  $V_{BE}$  (low  $I_C$ ). From (66), it can be obtained that

$$V_{BE} = R_{EB} \cdot I_C - \phi \cdot (T_j - T_0) + \eta \cdot V_{T0} \cdot \ln \frac{I_C}{A_E \cdot J_{S0}} \quad (68)$$

while the  $V_{BE}$  determined by extrapolating the low-current behavior (referred to as  $V_{BELC}$ ) can be derived from (67) as

$$V_{BELC} = \eta \cdot V_{T0} \cdot \ln \frac{I_C}{A_E \cdot J_{S0}} \quad (69)$$

The deviation of the measured  $V_{BE}$  from  $V_{BELC}$  can be obtained by subtracting (69) from (68):

$$\Delta V_{BE} = V_{BE} - V_{BELC} = R_{EB} \cdot I_C - \phi \cdot (T_j - T_0) \tag{70}$$

Using (18) with  $T_B = T_0$ , (70) can be rewritten as

$$\Delta V_{BE} = R_{EB} \cdot I_C - \phi \cdot R_{TH} \cdot P_D \tag{71}$$

where the  $I_C$  dependence of coefficient  $\phi$  has been determined in the first step of the procedure.

Pfost et al. measure the  $I_C$ - $V_{BE}$  curves at  $T_B = T_0$  applying various  $V_{CE}$  values. Then they select a quite high current  $I_C$  (which should in principle be low enough to avoid high-injection effects) and obtain the experimental  $\Delta V_{BE}$  vs.  $P_D$  behavior ( $P_D$  being approximatively given by  $I_C \cdot V_{CE}$ ) at  $I_C$ . By extrapolating the behavior to  $P_D \rightarrow 0$  W,  $R_{EB} \cdot I_C$  can be assessed, from which ( $I_C$  being assigned)  $R_{EB}$  is also determined. Then, they consider that (71) can be rearranged as

$$R_{TH} = \frac{R_{EB} \cdot I_C - \Delta V_{BE}}{\phi(I_C) \cdot P_D} \tag{72}$$

As  $\phi$  is known for the assigned  $I_C$ , and  $R_{EB}$  has been estimated,  $R_{TH}(T_0, P_D)$  can be obtained by using the given  $P_D$  and the measured  $\Delta V_{BE}$  values in (72).

For the InGaP/GaAs HBT, the extracted  $\phi'$  at  $I_C = 8$  mA was 1.174 mV/K (higher than  $\phi = 1.16$  mV/K since the nonlinear thermal effect due to the  $T_B$  increase prevails over the linear self-heating). Concerning the further step for the  $R_{TH}$  assessment, it must be remarked that the measurement of the  $T_B = T_0$   $V_{CE}$ -constant  $I_C$ - $V_{BE}$  curves by sweeping  $V_{BE}$  is critical, especially at high  $V_{CE}$ , as the marked self-heating may give rise to an irreversibly destructive thermal runaway (or equivalently to a flyback followed by a negative differential resistance branch by sweeping  $I_C$  [1,3]). In this technology,  $\Delta V_{BE}$  given by (71) is negative for each  $V_{CE}$  (each  $P_D$  at  $I_C = 8$  mA) since the self-heating prevails over the resistive effect. The  $R_{EB}$  value is assessed with very good accuracy. The extracted  $R_{TH}(T_0, P_D)$  vs.  $P_D$  is compared to the target (32) in Figure 3a; in the narrow  $P_D$  range analyzable in this approach, the  $R_{TH}$  increase dictated by the nonlinear self-heating effect is not accurately described, which can be attributed to the sensitivity of the method to the  $V_{BE}$  values to be identified on the  $V_{CE}$ -constant  $T_B = T_0$   $I_C$ - $V_{BE}$  curves at a chosen  $I_C$ . Anyway, the error corresponding to a given  $P_D$  is not so high.

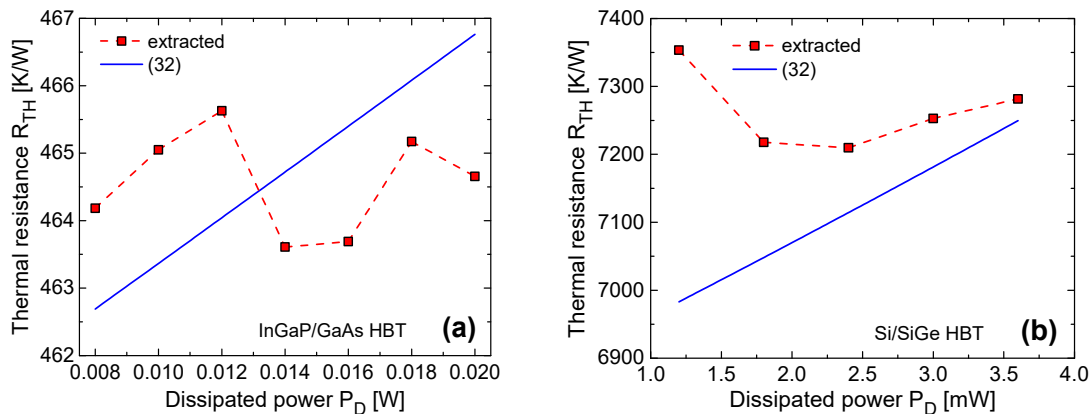


**Figure 3.**  $R_{TH}$  vs.  $P_D$  at  $T_B = T_0$ ; data extracted with the technique of Pfost et al. (dashed red lines with symbols) are compared to the target counterparts obtained from (32) (solid blue). (a) InGaP/GaAs HBT; (b) Si/SiGe HBT.

For the Si/SiGe HBT,  $I_C = 3$  mA was chosen to apply the procedure. A lower  $I_C$  would lead to problems in identifying the  $V_{BE}$  values on the  $V_{CE}$ -constant  $I_C$ - $V_{BE}$  curves.

Unfortunately, at this  $I_C$  the high-injection and nonlinear self-heating effects play a role. Coefficient  $\phi'$  was extracted to be 0.696 mV/K (higher than  $\phi = 0.675$  mV/K since the nonlinear thermal effect due to  $T_B$  dominates). In this technology,  $\Delta V_{BE}$  given by (71) is instead positive for each  $V_{CE}$  due to the prevailing resistive effect. The  $R_{EB}$  value is not properly extracted, as the high-injection effects, not included in (66) and thus (72), are misinterpreted as an additional resistive contribution. Due to the overestimated aggregate voltage drop  $R_{EB} \cdot I_C$ , the extracted  $R_{TH}(T_0, P_D)$  is higher than the target counterpart given by (32), as shown in Figure 3b.

4.5. Rieh et al. [7,27]

Rieh et al. [7,27] perform common-base measurements on a transistor with a directly-accessible emitter pad. First,  $I_E$  and  $V_{CB}$  are assigned,  $T_B$  is swept in a range of practical interest, and  $V_{BE}$  is measured, so that the  $I_E$ - and  $V_{CB}$ -constant  $V_{BE}-T_B$  curve is available. Then the transistor is biased with the same  $I_E$ ,  $T_B = T_0$  is applied,  $V_{CB}$  is increased, and  $V_{BE}$ ,  $I_B$  are measured; this allows obtaining the  $I_E$ -constant  $V_{BE}-V_{CB}$  curve, and, calculating  $P_D$  as  $I_E \cdot V_{BE} + (I_E - I_B) \cdot V_{CB}$ , also the corresponding  $V_{BE}-P_D$  characteristic. The two datasets can then be combined; more specifically,  $V_{BE}$  is eliminated to obtain  $T_B$  as a function of  $P_D$ .

From a mathematical point of view, the approach is articulated as follows. It was found that in the absence of avalanche, assuming temperature-insensitive parasitic resistances, and neglecting the drop  $R_B \cdot [I_B(T_j) - I_B(T_0)]$ , (16) holds. From (16), the  $V_{CB}$ - and  $I_E$ -constant  $V_{BE}-T_B$  curve can be modeled by (53), which inherently accounts for self-heating and the nonlinear thermal effect due to  $T_B$ . By neglecting self-heating, (53) reduces to

$$V_{BE} \approx V_{BE}(T_B = T_0) - \phi \cdot (T_B - T_0) \tag{73}$$

In the second measurement, by disregarding the nonlinear self-heating effect, (36) is obtained. By combining (36) and (73)

$$V_{BE}(T_B = T_0) - \phi \cdot (T_B - T_0) = V_{BE}(T_0) - \phi \cdot R_{TH} \cdot P_D \tag{74}$$

whence the experimental  $T_B-P_D$  curve is described by

$$T_B = T_0 - \frac{V_{BE}(T_0) - V_{BE}(T_B = T_0)}{\phi} + R_{TH} \cdot P_D \tag{75}$$

On the basis of (75),  $R_{TH}$  is obtained as the slope of the straight line fitting this curve, as shown in Figure 4.

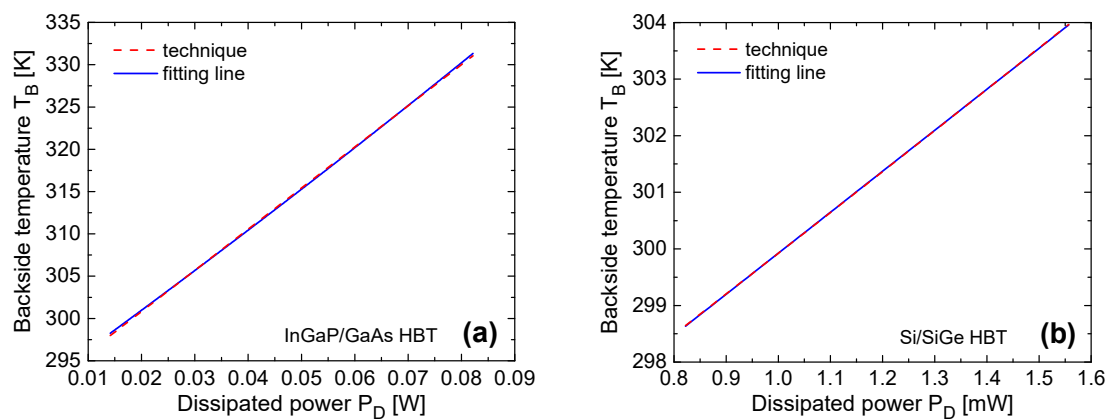


**Figure 4.** Backside temperature  $T_B$  vs.  $P_D$  resulting from the procedure proposed by Rieh et al. (dashed red lines);  $R_{TH}$  is obtained as the slope of the fitting line (solid blue). (a) InGaP/GaAs HBT; (b) Si/SiGe HBT.

Subsequently, Rieh et al. use the following procedure to obtain the  $T_j-P_D$  behavior starting from the available  $T_B-P_D$  one. First, they note that the above straight line intercepts the  $y$ -axis ( $P_D \rightarrow 0$  W) at a  $T_B$  value  $< T_0$ , referred to as  $T_B(P_D = 0$  W); then, they consider that the desired  $T_j-P_D$  curve would intercept the  $y$ -axis at  $T_j = T_0$ ; hence, they simply add  $T_0 - T_B(P_D = 0$  W) to the  $T_B-P_D$  curve to achieve the  $T_j-P_D$  counterpart.

Critical points of the technique are listed below:

- To eliminate  $V_{BE}$ , an interpolation process leading to the same  $V_{BE}$  values (i) in the  $I_E$ - and  $V_{CB}$ -constant  $V_{BE}-T_B$  data and (ii) in the  $I_E$ -constant  $V_{BE}-P_D$  data at  $T_B = T_0$  is needed.
- As noted by Vanhoucke et al. [29] and also by Rieh and his co-workers in [7], (73) is not correct due to the self-heating (and the  $T_B$ -induced nonlinear thermal effect) occurring during the measurement of the  $I_E$ - and  $V_{CB}$ -constant  $V_{BE}-T_B$  curve.
- The presence of the Early and of the nonlinear self-heating effect during the second measurement might lead to an  $R_{TH}$  overestimation.

For the InGaP/GaAs HBT,  $I_E = 10$  mA and  $V_{CB} = 0.5$  V were applied during the first measurement, and the same  $I_E$  value was adopted for the second measurement. Coefficient  $\phi'$ , extracted over a  $T_B$  span from 300 to 400 K, turned out to be 1.164 mV/K (higher than  $\phi = 1.141$  mV/K as the nonlinear thermal effect due to  $T_B$  prevails over the linear self-heating). Despite this,  $R_{TH}$  was extracted to be 468 K/W by limiting the  $P_D$  range to 0.03 W (with an error of 1.74% compared to  $R_{TH00}$ ) and 486.3 K/W by limiting the  $P_D$  range to 0.082 W (with an error of 5.7%) due to the nonlinear self-heating effect during the second measurement.

For the Si/SiGe HBT,  $I_E = 1$  mA and  $V_{CB} = 0.2$  V were applied during the first measurement. Coefficient  $\phi'$  was extracted to be 0.849 mV/K (higher than  $\phi = 0.829$  mV/K). The extracted  $R_{TH}$  was 7241 K/W by superiorly limiting the  $P_D$  range to 1.55 mW (with an error of 5.62% with respect to  $R_{TH00}$ ) due to the Early and the nonlinear self-heating effect in the second measurement. This conclusion was supported by a further analysis performed by removing *ad hoc* the Early effect from the Si/SiGe HBT model and limiting the  $R_{TH}$  extraction to  $P_D = 1.3$  mW; using the resulting synthetic data, the extracted  $R_{TH}$  was 6940 K/W (with an error of 1.23% with respect to  $R_{TH00}$ ).

#### 4.6. Vanhoucke et al. [29]

Vanhoucke et al. [29] recognize that during the first measurement the transistor can be affected by self-heating; as a consequence, they assume that the  $I_E$ - and  $V_{CB}$ -constant  $V_{BE}-T_B$  can be well approximated by a straight line described by (41), while the  $I_E$ -constant  $V_{BE}-P_D$  curve at  $T_B = T_0$  can be modeled using (36). By eliminating  $V_{BE}$  from (41) and (36), it is obtained that

$$T_B = T_0 + (1 + \phi \cdot R_{TH} \cdot I_E) \cdot \left[ -\frac{V_{BE}(T_0) - V_{BE}(T_B = T_0)}{\phi} + R_{TH} \cdot P_D \right] \tag{76}$$

where  $V_{BE}(T_0) = V_{BE}(T_j = T_0)$ . From (76), it can be easily inferred that  $R_{TH}$  is *not* given by the slope of the experimental  $T_B-P_D$  characteristic, as described by Rieh and his co-authors [7,27]. Vanhoucke et al. suggest improving the  $R_{TH}$  estimation as follows. From the knowledge of  $\phi' = \frac{\phi}{1 + \phi \cdot R_{TH} \cdot I_E}$  and  $\nu = -\phi \cdot R_{TH}$  (negative slope of the straight line ensuring the best fit with the  $V_{BE}-P_D$  curve),  $\phi$  can be eliminated to obtain

$$\phi' = \frac{-\frac{\nu}{R_{TH}}}{1 - \nu \cdot I_E} = \frac{|\nu|}{R_{TH} \cdot (1 + |\nu| \cdot I_E)} \tag{77}$$

whence  $R_{TH}$  is calculated as

$$R_{TH} = \frac{-\nu}{\phi' \cdot (1 - \nu \cdot I_E)} = \frac{|\nu|}{\phi' \cdot (1 + |\nu| \cdot I_E)} \tag{78}$$

For the InGaP/GaAs HBT, again  $I_E = 10$  mA and  $V_{CB} = 0.5$  V were applied during the first measurement, and the same  $I_E$  value was applied during the second measurement. Clearly, the extracted  $\phi'$  value does not change compared to Rieh et al. ( $=1.165$  mV/K), while the  $R_{TH}$  values slightly reduce: 465.5 and 483.6 K/W by limiting the  $P_D$  range to 0.03 and 0.09 W, respectively.

For the Si/SiGe HBT, again  $I_E = 1$  mA and  $V_{CB} = 0.2$  V were applied during the first measurement. Coefficient  $\phi'$  was equal to 0.849 mV/K. The extracted  $R_{TH}$  was 7196 K/W by limiting the  $P_D$  range to 1.55 mW.

It must be noted that in practice the slight accuracy improvement obtained with this technique is due to an unintentional increase of the error associated to the first measurement, where  $\phi'$  is assumed to be lower than  $\phi$  (while being actually *higher*), so that the inaccuracy corresponding to the second measurement is better compensated.

#### 4.7. University of Bordeaux

A thermometer-based technique relying on DC measurements was conceived and applied at University of Bordeaux, as reported in some PhD theses (e.g., [30]). Measurements are performed on a bipolar transistor in a GSG configuration. The base current  $I_B$  is kept constant,  $V_{CE}$  is swept, and  $V_{BE}$ ,  $I_C$  are measured at various  $T_B$  values. By evaluating the dissipated power  $P_D$  with (19), it is possible to plot the  $I_B$ -constant  $V_{BE}$ - $P_D$  curves at all the applied  $T_B$ , and, choosing a specific  $V_{BE}$ , the  $I_B$ - and  $V_{BE}$ -constant  $T_B$ - $P_D$  characteristic can be derived. Let us then consider that from (18)

$$T_B = T_j - R_{TH} \cdot P_D \quad (79)$$

By arbitrarily assuming  $T_j$  constant along this characteristic,  $R_{TH}$  can be determined from the slope.

For the InGaP/GaAs HBT,  $I_B$  was chosen equal to 0.7 mA and  $V_{BE}$  equal to 1.3 V; lower  $V_{BE}$  values would have pushed the  $P_D$  range under analysis to higher values, thus aggravating the nonlinear self-heating effect. The extracted  $R_{TH}$  was found to be 488 K/W, higher than  $R_{TH00}$  due to the slightly decreasing  $T_j$  along the curve and to the nonlinear self-heating effect.

For the Si/SiGe HBT,  $I_B$  was chosen equal to 20  $\mu$ A and  $V_{BE}$  equal to 0.88 V; choosing a lower  $I_B$  does not allow applying the technique, as it is impossible to find a  $V_{BE}$  at which two avalanche-free points can be intercepted. The extracted  $R_{TH}$  was found to be 7278 K/W considering the  $T_B$  span from 300 to 340 K, and 7424 K/W considering the  $T_B$  span from 300 to 360 K, as dictated by the slight  $T_j$  decrease along the  $T_B$ - $P_D$  curve and to the nonlinear self-heating effect.

#### 4.8. d'Alessandro et al. [18,31]

The technique developed by d'Alessandro et al. [18] is articulated as follows. Given a bipolar transistor with accessible emitter operated in common-base configuration, the  $V_{CB}$ - and  $I_E$ -constant  $V_{BE}$ - $T_B$  characteristic is measured at *very low*  $I_E$ . Under these conditions, the self-heating (and thus the nonlinear thermal effect due to  $T_B$ ) can be *safely* neglected; consequently, (53) reduces to (73). Hence, coefficient  $\phi$  can be extracted at the applied  $I_E$ . The measurement is then repeated at other, *very low* as well,  $I_E$  values. Hence, the experimental  $\phi$  vs.  $I_E$  behavior is obtained, and parameter  $\phi_0$  of the logarithmic law (17) can be easily calibrated. In [18], it has been demonstrated that, for a given technology node,  $\phi_0$  is almost independent of the transistor layout, in accordance with the theory formulated in Section 2. The accuracy of the  $\phi_0$  calibration is verified through the following procedure. In the absence of avalanche, Early, high-injection, and resistive effects, (20) reduces to

$$I_C \approx A_E \cdot J_{S0} \cdot \exp \left[ \frac{V_{BE} + \phi \cdot (T_j - T_0)}{\eta \cdot V_{T0}} \right] \quad (80)$$

If the self-heating is negligible, (80) becomes:

$$I_C \approx A_E \cdot J_{S0} \cdot \exp \left[ \frac{V_{BE} + \phi \cdot (T_B - T_0)}{\eta \cdot V_{T0}} \right] \quad (81)$$

Here,  $\phi$  is a function of  $I_E$  according to (17). Considering that  $I_E \approx I_C$ , (17) can be rewritten as

$$\phi = \phi_0 - \eta \cdot \frac{k}{q} \cdot \ln \frac{I_C}{A_E \cdot J_{S0}} \quad (82)$$

Substituting (82) into (81), it is obtained that

$$\frac{I_C}{A_E \cdot J_{S0}} = \exp \left[ \frac{V_{BE} + \phi_0 \cdot (T_B - T_0) - \eta \cdot \frac{k}{q} \cdot (T_B - T_0) \cdot \ln \frac{I_C}{A_E \cdot J_{S0}}}{\eta \cdot V_{T0}} \right] \quad (83)$$

By applying the logarithm to both sides of (83),

$$\eta \cdot V_{T0} \cdot \ln \frac{I_C}{A_E \cdot J_{S0}} = V_{BE} + \phi_0 \cdot (T_B - T_0) - \eta \cdot \frac{k}{q} \cdot (T_B - T_0) \cdot \ln \frac{I_C}{A_E \cdot J_{S0}} \quad (84)$$

whence

$$I_C = A_E \cdot J_{S0} \cdot \exp \left[ \frac{V_{BE} + \phi_0 \cdot (T_B - T_0)}{\eta \cdot V_{T0} + \eta \cdot \frac{k}{q} \cdot (T_B - T_0)} \right] = A_E \cdot J_{S0} \cdot \exp \left[ \frac{V_{BE} + \phi_0 \cdot (T_B - T_0)}{\eta \cdot \frac{kT_B}{q}} \right] \quad (85)$$

If the experimental  $V_{CE}$ -constant (with low  $V_{CE}$ )  $I_C$ - $V_{BE}$  curves measured at various  $T_B$  are favorably described by (85) with optimized  $\phi_0$  at low  $V_{BE}$  (low  $I_C$ ), the accuracy of the calibration is verified [18,19].

Once  $\phi_0$  is calibrated, (17) can be exploited to determine  $\phi$  for higher  $I_E$  values, thus avoiding all the mechanisms leading to the extraction of a  $\phi'$  different from  $\phi$ ; improved accuracy at particularly high  $I_E$  values can be obtained using (14), which however requires a preliminary calibration of parameters  $J_{HI}$  and  $n_{HI}$ . To summarize, this technique solves all the issues associated to the thermometer calibration, as it allows an accurate evaluation of the  $\phi$  value corresponding to the  $I_E$  to be used in the second measurement.

As usual, the second measurement is performed at  $T_B = T_0$  by forcing an  $I_E$  value high enough to entail perceptible self-heating, and  $V_{CB}$  is increased; the  $I_E$  value and the  $V_{CB}$  range should not lead to significant nonlinear self-heating effect to allow the extraction of an  $R_{TH}$  close to  $R_{TH00}$ . In this case, (36) is assumed to be valid. From simple elaboration of the experimental data,  $V_{BE}$  is obtained as a function of  $P_D$ , the  $V_{BE}$ - $P_D$  behavior is almost linear, with a slope  $\nu = -\phi \cdot R_{TH}$ , and  $R_{TH}$  is calculated with (38).

As an equivalent alternative, the measured  $V_{BE}$ - $V_{CB}$  data can be directly used without further elaboration. Let us consider that (36) can be recast as

$$V_{BE} \approx V_{BE}(T_0) - \phi \cdot R_{TH} \cdot I_E \cdot (V_{BE} + V_{CB}) \quad (86)$$

from which

$$V_{BE} = \frac{V_{BE}(T_0)}{1 + \phi \cdot R_{TH} \cdot I_E} - \frac{\phi \cdot R_{TH} \cdot I_E}{1 + \phi \cdot R_{TH} \cdot I_E} \cdot V_{CB} \quad (87)$$

where  $\phi$  at the selected  $I_E$  is computed with (17) or (14). As can be seen, the  $I_E$ -constant  $V_{BE}$ - $V_{CB}$  behavior is also expected to be linear. By extracting the (negative) slope  $\gamma$  of the straight line ensuring the best matching with experimental data,  $R_{TH}$  can be calculated as

$$R_{TH} = \frac{|\gamma|}{\phi \cdot I_E \cdot (1 - |\gamma|)} \quad (88)$$

For the InGaP/GaAs HBT, the extracted  $R_{TH}$  was equal to 476.5 K/W at  $I_E = 10$  mA by superiorly limiting  $V_{CB}$  to 2.3 V (with an error of 3.59% compared to  $R_{TH00}$  due to the nonlinear self-heating effect in the second measurement). It can be inferred that the error is paradoxically *higher* than that corresponding to less elaborate techniques since in this case coefficient  $\phi$  is well evaluated, and the compensation of errors does not take place.

For the Si/SiGe HBT, the extracted  $R_{TH}$  was equal to 7412.6 K/W at  $I_E = 1$  mA by limiting  $V_{CB}$  to 0.75 V (with an error of 8.12% with respect to  $R_{TH00}$ ), which is due to the Early and the nonlinear self-heating effect, as well as to the absence of compensation of errors. Removing *ad hoc* the Early effect from the HBT model, and repeating the extraction on the new synthetic data,  $R_{TH} = 7104.7$  K/W by limiting the simulation to  $V_{CB} = 0.5$  V (with an error of 3.63%).

Improved variants of the technique by d’Alessandro et al. were developed to purify the  $R_{TH}$  extraction from the Early effect [31], which is expected to play a relevant role in PNP HBTs and in Si bipolar junction transistors (BJTs), regardless of their application. For the sake of brevity, here we describe only the first approach, which requires the preliminary determination of  $V_{AF}$  from common-emitter  $I_C$ - $V_{CE}$  measurements; another strategy presented in [31,56] and inspired by an early paper of Sparkes [62] is not based on the knowledge of  $V_{AF}$ .

Making use of (19), (52) can be rewritten as ( $I_C \approx I_E$ ):

$$V_{BE} \approx R_{EB} \cdot I_E + \eta \cdot V_{T0} \cdot \ln \frac{I_E}{\left(1 + \frac{V_{CB}}{V_{AF}}\right) \cdot A_E \cdot J_{S0}} - \phi \cdot R_{TH} \cdot I_E \cdot (V_{BE} + V_{CB}) \quad (89)$$

from which

$$V_{BE} = \frac{1}{1 + \phi \cdot R_{TH} \cdot I_E} \cdot \left[ R_{EB} \cdot I_E - \phi \cdot R_{TH} \cdot I_E \cdot V_{CB} + \eta \cdot V_{T0} \cdot \ln \frac{I_E}{\left(1 + \frac{V_{CB}}{V_{AF}}\right) \cdot A_E \cdot J_{S0}} \right] \quad (90)$$

Hence, the  $I_E$ -constant  $V_{BE}$ - $V_{CB}$  behavior at  $T_B = T_0$  is still nearly linear, with an absolute value  $|\gamma|$  of the slope higher than that in the absence of the Early effect, and approximately given by

$$|\gamma| \approx \frac{\phi \cdot R_{TH} \cdot I_E}{1 + \phi \cdot R_{TH} \cdot I_E} + \frac{1}{1 + \phi \cdot R_{TH} \cdot I_E} \cdot \frac{\eta \cdot V_{T0}}{V_{AF}} \quad (91)$$

Once  $|\gamma|$  is extracted,  $R_{TH}$  is easily determined as

$$R_{TH} = \frac{|\gamma| - \frac{\eta \cdot V_{T0}}{V_{AF}}}{(1 - |\gamma|) \cdot \phi \cdot I_E} \quad (92)$$

Exploiting this approach for the Si/SiGe HBT (where  $V_{AF} = 110$  V), the extracted  $R_{TH}$  was equal to 7113 K/W.

#### 4.9. Summary of the Main Findings

Some techniques like those developed by Dawson et al. [24], Rieh et al. [7,27], and Vanhoucke et al. [29] are based on a first measurement aimed at calibrating the thermometer, which, if the emitter pad is accessible, is performed by assigning  $I_E$  and  $V_{CB}$ , measuring  $V_{BE}$  as a function of  $T_B$ , and extracting the absolute value  $\phi'$  of the slope of the straight line ensuring the best fit with experimental data. Then, the  $R_{TH}$  assessment is carried out by measuring  $V_{BE}$  as a function of  $P_D$  (or equivalently as a function of  $V_{CB}$ ) by keeping  $I_E$  constant at the same value as in the first measurement and  $T_B = T_0$ , extracting the (negative) slope  $\nu$  of the straight line providing the best alignment with the  $V_{BE}$ - $P_D$  characteristic (or equivalently the slope  $\gamma$  of the straight line matching with the  $V_{BE}$ - $V_{CB}$  characteristic), and elaborating this slope with the temperature coefficient  $\phi$  of the “internal” base-emitter voltage  $V_{BEj}$ .

Unfortunately, the techniques of Dawson et al. [24] and Rieh et al. [7,27] are based on the assumption that the extracted  $\phi'$  coincides with  $\phi$ . Since the chosen  $I_E$  is expected to trigger a perceptible self-heating in the second measurement, self-heating will also take place in the first measurement, even though  $V_{CB}$  is low. In the ideal absence of nonlinear thermal effects, the linear self-heating would lead to  $\phi' < \phi$ . Instead, the increase in  $R_{TH}$  induced by the  $T_B$  sweep implies that  $\phi' > \phi$ ; moreover, the higher is the  $T_B$  range, the higher  $\phi'$ . Using  $\phi'$  in combination with  $|\nu|$  (or  $|\gamma|$ ) for the final thermal resistance evaluation could in principle give rise to an underestimation of  $R_{TH}$ .

In the second measurement, two mechanisms deserve attention. First, the Early effect can be misinterpreted as an additional overheating and thus could lead to an overestimation of  $R_{TH}$ . Second, the nonlinear self-heating effect due to the increase in  $P_D$  makes the thermal resistance grow along the  $V_{BE}-P_D$  (or  $V_{BE}-V_{CB}$ ) curve. Consequently, although  $\phi'$  is higher than  $\phi$ , the extracted  $R_{TH}$  is always higher than  $R_{TH00}$ . This overestimation is exacerbated when the extraction of  $\nu$  (or  $\gamma$ ) is performed over a larger  $P_D$  (or  $V_{CB}$ ) range; hence, if the aim is to assess  $R_{TH00}$ , the maximum  $P_D$  (or  $V_{CB}$ ) should be selected as small as possible.

Paradoxically, the adoption of  $\phi' > \phi$  in the elaboration for the  $R_{TH}$  assessment mitigates the above overestimation, that is, the accuracy improves due to a compensation of errors.

Vanhoucke et al. [29] disregard the nonlinear thermal effect due to  $T_B$  in the first measurement, and thus assume that  $\phi' < \phi$  due to the linear self-heating, which would in principle lead to an  $R_{TH}$  overestimation. Owing to this, they conceive an improved formula to evaluate  $R_{TH}$  from  $|\nu|$  and  $\phi'$  that accounts for the self-heating in the first measurement, and extract an  $R_{TH}$  slightly lower than that obtained by Dawson et al. [24] and Rieh et al. [7,27]. However, in practice  $\phi' > \phi$ , so the technique of Vanhoucke et al. [29] unintentionally exacerbates the error associated to the first measurement, and thus allows obtaining a slightly higher accuracy in the  $R_{TH}$  evaluation due to a more marked compensation of errors.

The technique of d'Alessandro et al. [18] allows solving the self-heating issue related to the first measurement by determining an accurate  $\phi$  model as a function of the applied emitter current  $I_E$ . Unfortunately, in the basic approach, the resulting error is higher than that obtained with other techniques, as the discrepancy between  $R_{TH}$  and  $R_{TH00}$  due to the Early and the nonlinear self-heating effect is no longer compensated by the error made in the thermometer calibration. Improved variants of the technique allow purifying the result from the impact of the Early effect.

Among the techniques aimed at determining the impact of nonlinear thermal effects on  $R_{TH}$ , namely, those developed by Bovolon et al. [25] and Yeats [26] for the whole  $R_{TH}(T_B, P_D)$  behavior, and Pfof et al. [28] for the  $R_{TH}(T_0, P_D)$  behavior, the one of Yeats has been found to be very accurate when applied to simulated data. However, in practice this technique is very sensitive to the measured  $V_{BE}$  values, as it is based on the direct use of the thermometer to find the junction temperature  $T_j$  and then the  $R_{TH}$  at the assigned  $I_E$ . Consequently, noisy  $V_{BE}$  data are expected to perceptibly affect the  $R_{TH}$  extraction despite the polynomial fitting. The method by Pfof et al. is cumbersome to apply to experimental data, as it is based on the detection of points at the same  $I_C$  on various  $I_C-V_{BE}$  characteristics at  $T_B = T_0$  and different  $V_{CE}$  values; as this detection must be carried out at high  $I_C$ , the extraction accuracy can be affected by high-injection effects, and in some critical cases the HBT could be even destroyed by the occurrence of a thermal runaway. All these considerations are summarized in Table 3 and sketched in Figure 5, which illustrates the main features of the investigated techniques and the correlations among them as a function of the year of publication.

**Table 3.** Main features of the thermometer-based  $R_{TH}$  extraction techniques.

Technique	Advantages, Approximations, and Limitations
Dawson et al. [24] and Rieh et al. [7,27]	The technique developed by Rieh et al. can be considered a variant of the classical approach of Dawson et al., the latter being more complex as it is applied to a device with grounded emitter, and the first being simpler as it is applied to a device with accessible emitter, for which it is possible to force an assigned emitter current. In both techniques, coefficient $\phi'$ extracted in the first measurement is higher than the desired $\phi$ due to the nonlinear thermal effect induced by the $T_B$ increase on the $R_{TH}$ . Conveniently, the resulting error (which would give rise to an $R_{TH}$ underestimation) is compensated by another error in the second measurement dictated by the Early and nonlinear self-heating effects (such an error tends to overestimate $R_{TH}$ ). By keeping $I_E$ sufficiently low in both measurements and choosing a limited $P_D$ range in the second measurement, these techniques allow extracting $R_{TH00}$ with a fairly good accuracy for the InGaP/GaAs and Si/SiGe HBT devices under test, which do not exhibit a significant Early effect. However, it must be remarked that this accuracy originates from a compensation of errors; hence, further analyses should be performed to establish if a similar compensation takes place also in other HBT technologies devised for RF applications.
Bovolon et al. [25]	This technique can be reviewed as an extension of the differential variant of the approach of Dawson et al. conceived to extract $R_{TH}$ as a function of $T_B$ and $P_D$ . Unfortunately, due to its differential nature and to the underlying assumptions, this technique suffers from a marked inaccuracy in describing the impact of the nonlinear self-heating effect, regardless of the HBT technology.
Yeats [26]	This technique represents an extension of the approaches of Dawson et al. and Rieh et al. aimed to extract $R_{TH}$ vs. $T_B$ and $P_D$ . The method allows determining accurate results when applied to simulated data (corresponding to <i>ideal</i> noiseless measurements). However, as the approach is based on the direct use of the thermometer to evaluate the junction temperature $T_j$ , noisy $V_{BE}$ data coming from <i>real</i> measurements are expected to jeopardize the extraction accuracy.
Pfost et al. [28]	This approach is developed to extract the $R_{TH}$ dependence on $P_D$ at $T_B = T_0$ ; differently from other techniques, the method operates on $I_C$ - $V_{BE}$ characteristics and is quite critical, as it is based on the detection of points at the same $I_C$ on characteristics measured at different $V_{CE}$ values. This detection is indeed possible when $I_C$ ( $V_{BE}$ ) is high, but in severe cases increasing $V_{BE}$ can lead to thermal runaway, and in milder cases the extraction accuracy can be affected by high-injection effects.
Vanhoucke et al. [29]	This technique is conceived to improve the approaches of Dawson et al. and Rieh et al. by mitigating the error due to self-heating in the first measurement. However, Vanhoucke et al. improperly assume that only <i>linear</i> self-heating takes place, while the prevailing mechanism is the $R_{TH}$ increase due to the <i>nonlinear</i> thermal effect induced by the $T_B$ sweep. Hence, this technique unintentionally exacerbates the error associated to the first measurement, and paradoxically improves the compensation of errors, thus leading to a slightly higher accuracy in the $R_{TH00}$ extraction. Again, as the accuracy derives from a compensation of errors, it is difficult to predict what might happen by applying this method to other HBT technologies.
University of Bordeaux	This technique is based on common-emitter measurements performed at various $T_B$ values by sweeping $V_{CE}$ and keeping $I_B$ constant. By elaborating the results and selecting a $V_{BE}$ value, the $I_B$ - and $V_{BE}$ -constant $T_B$ - $P_D$ curve is obtained, and the $R_{TH}$ is determined from its slope. Unfortunately, the $I_B$ and $V_{BE}$ values are not simple to choose, which makes the method quite difficult to apply. For the HBT technologies under test, the extracted $R_{TH}$ is higher than $R_{TH00}$ due to an underlying approximation and to the nonlinear self-heating effect.
d'Alessandro et al. [18,31]	The technique in [18] aims to improve the accuracy in the extraction of coefficient $\phi$ with respect to the approaches of Dawson et al. and Rieh et al., the price to pay being an increased elaboration effort. Consequently, in this case the compensation of errors does not take place, and this technique overestimates $R_{TH}$ with respect to $R_{TH00}$ due to the nonlinear self-heating effect and the Early effect in the second measurement. The inaccuracy dictated by the nonlinear self-heating effect can be alleviated by limiting the $P_D$ range in which the $R_{TH}$ extraction is performed. The extended versions in [31] allow purifying the extraction from the Early effect, which is misinterpreted as additional self-heating. As a result, differently from all other techniques, the approaches in [31] can be adopted not only to NPN HBTs, but also to PNP HBTs and Si BJTs, where the Early effect plays a more relevant role.

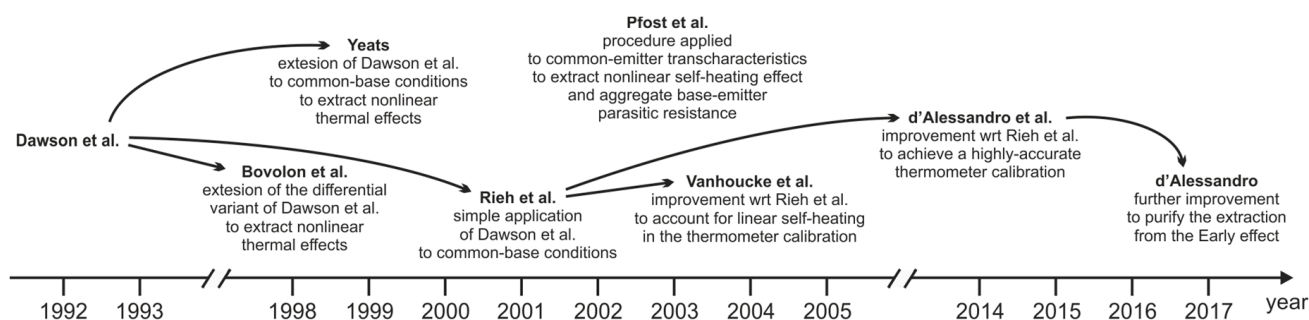


**Figure 5.** Representation of the analyzed extraction techniques, with emphasis on their key features, interrelations among them, and year of publication [7,18,24–26,28,29,31].

## 5. Conclusions

In this paper, a critical review of DC indirect techniques for the experimental extraction of the thermal resistance of bipolar transistors from straightforward current/voltage measurements has been presented. The accuracy verification has been performed by (i) simulating the DC characteristics of the devices under test through PSPICE electrothermal simulation of a simple, yet accurate enough, transistor model, (ii) applying the techniques to the current/voltage data, and (iii) comparing the extracted thermal resistance to the target one implemented in the transistor model. The impact of both nonlinear thermal effects has been explained in detail. An InGaP/GaAs HBT and a Si/SiGe HBT for high-frequency applications have been selected as case-studies. Results obtained by performing Keysight ADS simulations of compact transistor models such as AgilentHBT and HICUM also for other HBT technologies are in line with those shown and discussed in this paper.

**Author Contributions:** Methodology, V.d.; Software, V.d., A.P.C., C.S. and L.C.; Investigation, V.d., M.M., M.S. and P.J.Z.; Writing—Original Draft Preparation, V.d.; Writing—Review and Editing, V.d.; Supervision, V.d., A.P.C., C.S., M.M., M.S. and P.J.Z. All authors have read and agreed to the published version of the manuscript.

**Funding:** This research received no external funding.

**Data Availability Statement:** Not applicable.

**Acknowledgments:** This work is dedicated to the memory of Niccolò Rinaldi, a bright Researcher who prematurely passed away in 2018.

**Conflicts of Interest:** The authors declare no conflict of interest.

## References

1. Nenadović, N.; d'Alessandro, V.; Nanver, L.K.; Tamigi, F.; Rinaldi, N.; Slotboom, J.W. A back-wafer contacted silicon-on-glass integrated bipolar process—Part II: A novel analysis of thermal breakdown. *IEEE Trans. Electron Devices* **2004**, *51*, 51–62. [[CrossRef](#)]
2. Rinaldi, N.; d'Alessandro, V. Theory of electrothermal behavior of bipolar transistors: Part I—Single-finger devices. *IEEE Trans. Electron Devices* **2005**, *52*, 2009–2021. [[CrossRef](#)]
3. La Spina, L.; d'Alessandro, V.; Russo, S.; Rinaldi, N.; Nanver, L.K. Influence of concurrent electrothermal and avalanche effects on the safe operating area of multifinger bipolar transistors. *IEEE Trans. Electron Devices* **2009**, *56*, 483–491. [[CrossRef](#)]
4. Lee, C.-P.; Tao, N.G.M.; Lin, B.J.-F. Studies of safe operating area of InGaP/GaAs heterojunction bipolar transistors. *IEEE Trans. Electron Devices* **2014**, *61*, 943–949. [[CrossRef](#)]
5. Rinaldi, N. Small-signal operation of semiconductor devices including self-heating, with application to thermal characterization and instability analysis. *IEEE Trans. Electron Devices* **2001**, *48*, 323–331. [[CrossRef](#)]
6. Russo, S.; La Spina, L.; d'Alessandro, V.; Rinaldi, N.; Nanver, L.K. Influence of layout design and on-wafer heatspreaders on the thermal behavior of fully-isolated bipolar transistors: Part II—Dynamic analysis. *Solid-State Electron* **2010**, *54*, 754–762. [[CrossRef](#)]
7. Rieh, J.-S.; Greenberg, D.; Liu, Q.; Joseph, A.J.; Freeman, G.; Ahlgren, D.C. Structure optimization of trench-isolated SiGe HBTs for simultaneous improvements in thermal and electrical performances. *IEEE Trans. Electron Devices* **2005**, *52*, 2744–2752. [[CrossRef](#)]
8. Seiler, U.; Koenig, E.; Narozny, P.; Dämbkes, H. Thermally triggered collapse of collector current in power heterojunction bipolar transistors. In Proceedings of the IEEE Bipolar/BiCMOS Circuits and Technology Meeting (BCTM), Minneapolis, MN, USA, 4–5 October 1993; pp. 257–260.

9. Liu, W.; Nelson, S.; Hill, D.G.; Khatibzadeh, A. Current gain collapse in microwave multifinger heterojunction bipolar transistors operated at very high power densities. *IEEE Trans. Electron Devices* **1993**, *40*, 1917–1927. [[CrossRef](#)]
10. Liu, W.; Khatibzadeh, A. The collapse of current gain in multi-finger heterojunction bipolar transistors: Its substrate temperature dependence, instability criteria, and modeling. *IEEE Trans. Electron Devices* **1994**, *41*, 1698–1707. [[CrossRef](#)]
11. La Spina, L.; d’Alessandro, V.; Russo, S.; Nanver, L.K. Thermal design of multifinger bipolar transistors. *IEEE Trans. Electron Devices* **2010**, *57*, 1789–1800. [[CrossRef](#)]
12. Sevimli, O.; Parker, A.E.; Fattorini, A.P.; Mahon, S.J. Measurement and modeling of thermal behavior in InGaP/GaAs HBTs. *IEEE Trans. Electron Devices* **2013**, *60*, 1632–1639. [[CrossRef](#)]
13. d’Alessandro, V.; Catalano, A.P.; Magnani, A.; Codecasa, L.; Rinaldi, N.; Moser, B.; Zampardi, P.J. Simulation comparison of InGaP/GaAs HBT thermal performance in wire-bonding and flip-chip technologies. *Microelectron. Reliab.* **2017**, *78*, 233–242. [[CrossRef](#)]
14. d’Alessandro, V.; Catalano, A.P.; Codecasa, L.; Zampardi, P.J.; Moser, B. Accurate and efficient analysis of the upward heat flow in InGaP/GaAs HBTs through an automated FEM-based tool and Design of Experiments. *Int. J. Numer. Model. Electron. Netw. Devices Fields* **2019**, *32*, e2530. [[CrossRef](#)]
15. d’Alessandro, V.; Catalano, A.P.; Scognamillo, C.; Codecasa, L.; Zampardi, P.J. Analysis of electrothermal effects in devices and arrays in InGaP/GaAs HBT technology. *Electronics* **2021**, *10*, 757. [[CrossRef](#)]
16. d’Alessandro, V.; Marano, I.; Russo, S.; Céli, D.; Chantre, A.; Chevalier, P.; Pourchon, F.; Rinaldi, N. Impact of layout and technology parameters on the thermal resistance of SiGe:C HBTs. In Proceedings of the IEEE Bipolar/BiCMOS Circuits and Technology Meeting (BCTM), Austin, TX, USA, 4–6 October 2010; pp. 137–140.
17. Sahoo, A.K.; Frégonèse, S.; Weiß, M.; Malbert, N.; Zimmer, T. A scalable electrothermal model for transient self-heating effects in trench-isolated SiGe HBTs. *IEEE Trans. Electron Devices* **2012**, *59*, 2619–2625. [[CrossRef](#)]
18. d’Alessandro, V.; Sasso, G.; Rinaldi, N.; Aufinger, K. Influence of scaling and emitter layout on the thermal behavior of toward-THz SiGe:C HBTs. *IEEE Trans. Electron Devices* **2014**, *61*, 3386–3394. [[CrossRef](#)]
19. d’Alessandro, V.; Magnani, A.; Codecasa, L.; Rinaldi, N.; Aufinger, K. Advanced thermal simulation of SiGe:C HBTs including back-end-of-line. *Microelectron. Reliab.* **2016**, *67*, 38–45. [[CrossRef](#)]
20. Balanethiram, S.; Berkner, J.; D’Esposito, R.; Frégonèse, S.; Céli, D.; Zimmer, T. Extracting the temperature dependence of thermal resistance from temperature-controlled DC measurements of SiGe HBTs. In Proceedings of the IEEE Bipolar/BiCMOS Circuits and Technology Meeting (BCTM), Miami, FL, USA, 19–21 October 2017; pp. 94–97.
21. Balanethiram, S.; D’Esposito, R.; Frégonèse, S.; Chakravorty, A.; Zimmer, T. Validation of thermal resistance extracted from measurements on stripe geometry SiGe HBTs. *IEEE Trans. Electron Devices* **2019**, *66*, 4151–4155. [[CrossRef](#)]
22. Huszka, Z.; Nidhin, K.; Céli, D.; Chakravorty, A. Extraction of compact static thermal model parameters for SiGe HBTs. *IEEE Trans. Electron Devices* **2021**, *68*, 491–496. [[CrossRef](#)]
23. Waldrop, J.R.; Wang, K.C.; Asbeck, P.M. Determination of junction temperature in AlGaAs/GaAs heterojunction bipolar transistor by electrical measurement. *IEEE Trans. Electron Devices* **1992**, *39*, 1248–1250. [[CrossRef](#)]
24. Dawson, D.E.; Gupta, A.K.; Salib, M.L. CW measurements of HBT thermal resistance. *IEEE Trans. Electron Devices* **1992**, *39*, 2235–2239. [[CrossRef](#)]
25. Bovolon, N.; Baureis, P.; Müller, J.-E.; Zwicknagl, P.; Schultheis, R.; Zanoni, E. A simple method for the thermal resistance measurement of AlGaAs/GaAs heterojunction bipolar transistors. *IEEE Trans. Electron Devices* **1998**, *45*, 1846–1848. [[CrossRef](#)]
26. Yeats, B. Inclusion of topside metal heat spreading in the determination of HBT temperatures by electrical and geometrical methods. In Proceedings of the IEEE Gallium Arsenide Integrated Circuit (GaAs IC) Symposium, Monterey, CA, USA, 17–20 October 1999; pp. 59–62.
27. Rieh, J.-S.; Greenberg, D.; Jagannathan, B.; Freeman, G.; Subanna, S. Measurement and modeling of thermal resistance of high speed SiGe heterojunction bipolar transistors. In Proceedings of the IEEE Topical Meeting on Silicon Monolithic Integrated Circuits in RF Systems, Ann Arbor, MI, USA, 14 September 2001; pp. 110–113.
28. Pfost, M.; Kubrak, V.; Brenner, P. A practical method to extract the thermal resistance for heterojunction bipolar transistors. In Proceedings of the IEEE conference on European Solid-State Device Research (ESSDERC), Estoril, Portugal, 16–18 September 2003; pp. 335–338.
29. Vanhoucke, T.; Boots, H.M.J.; van Noort, W.D. Revised method for extraction of the thermal resistance applied to bulk and SOI SiGe HBTs. *IEEE Electron Device Lett.* **2004**, *25*, 150–152. [[CrossRef](#)]
30. Koné, G.A. Caractérisation des Effets Thermiques et des Mécanismes de Défaillance Spécifiques aux Transistors Bipolaires Submicroniques sur Substrat InP Dédiés aux Transmissions. Ph.D. Dissertation, University of Bordeaux 1, Bordeaux, France, 20 December 2011.
31. d’Alessandro, V. Experimental DC extraction of the thermal resistance of bipolar transistors taking into account the Early effect. *Solid-State Electron.* **2017**, *127*, 5–12. [[CrossRef](#)]
32. Liu, W.; Yuksel, A. Measurement of junction temperature of an AlGaAs/GaAs heterojunction bipolar transistor operating at large power densities. *IEEE Trans. Electron Devices* **1995**, *42*, 358–360. [[CrossRef](#)]
33. Marsh, S.P. Direct extraction technique to derive the junction temperature of HBT’s under high self-heating bias conditions. *IEEE Trans. Electron Devices* **2000**, *47*, 288–291. [[CrossRef](#)]

34. Berkner, J. Extraction of Thermal Resistance and Its Temperature Dependence Using DC Methods. In Proceedings of the HICUM Workshop, Dresden, Germany, 18–19 June 2007. Available online: [https://www.iet.tu-dresden.de/iet/eb/forsch/Models/workshop0607/contr/Berkner\\_Infineon\\_HICUM\\_WS\\_2007\\_Dresden\\_070621s.pdf](https://www.iet.tu-dresden.de/iet/eb/forsch/Models/workshop0607/contr/Berkner_Infineon_HICUM_WS_2007_Dresden_070621s.pdf) (accessed on 1 August 2022).
35. Reisch, M. Self-heating in BJT circuit parameter extraction. *Solid-State Electron.* **1992**, *35*, 677–679. [[CrossRef](#)]
36. Zweidinger, D.T.; Fox, R.M.; Brodsky, J.S.; Jung, T.; Lee, S.-G. Thermal impedance extraction for bipolar transistors. *IEEE Trans. Electron Devices* **1996**, *43*, 342–346. [[CrossRef](#)]
37. Tran, H.; Schröter, M.; Walkey, D.J.; Marchesan, D.; Smy, T.J. Simultaneous extraction of thermal and emitter series resistances in bipolar transistors. In Proceedings of the IEEE Bipolar/BiCMOS Circuits and Technology Meeting (BCTM), Minneapolis, MN, USA, 28–30 September 1997; pp. 170–173.
38. Williams, D.; Tasker, P. Thermal parameter extraction technique using DC I–V data for HBT transistors. In Proceedings of the IEEE High Frequency Postgraduate Student Colloquium, Dublin, Ireland, 7–8 September 2000; pp. 71–75.
39. Pawlak, A.; Lehmann, S.; Schröter, M. A simple and accurate method for extracting the emitter and thermal resistance of BJTs and HBTs. In Proceedings of the IEEE Bipolar/BiCMOS Circuits and Technology Meeting (BCTM), Coronado, CA, USA, 28 September–1 October 2014; pp. 175–178.
40. Menozzi, R.; Barrett, J.; Ersland, P. A new method to extract HBT thermal resistance and its temperature and power dependence. *IEEE Trans. Device Mater. Reliab.* **2005**, *5*, 595–601. [[CrossRef](#)]
41. Müller, M.; d’Alessandro, V.; Falk, S.; Weimer, C.; Jin, X.; Krattenmacher, M.; Kuthe, P.; Claus, M.; Schröter, M. Methods for extracting the temperature- and power-dependent thermal resistance for SiGe and III–V HBTs from DC measurements: A review and comparison across technologies. *IEEE Trans. Electron Devices* **2022**, *69*, 4064–4074. [[CrossRef](#)]
42. Rinaldi, N.; d’Alessandro, V. Theory of electrothermal behavior of bipolar transistors: Part III—Impact ionization. *IEEE Trans. Electron Devices* **2006**, *53*, 1683–1697. [[CrossRef](#)]
43. MacFarlane, G.G.; McLean, T.P.; Quarrington, J.E.; Roberts, V. Fine structure in the absorption-edge spectrum of Si. *Phys. Rev.* **1958**, *111*, 1245–1254. [[CrossRef](#)]
44. d’Alessandro, V.; Sasso, G.; Rinaldi, N.; Aufinger, K. Experimental DC extraction of the base resistance of bipolar transistors: Application to SiGe:C HBTs. *IEEE Trans. Electron Devices* **2016**, *63*, 2691–2699. [[CrossRef](#)]
45. d’Alessandro, V.; D’Esposito, R.; Metzger, A.G.; Kwok, K.H.; Aufinger, K.; Zimmer, T.; Rinaldi, N. Analysis of electrothermal and impact-ionization effects in bipolar cascode amplifiers. *IEEE Trans. Electron Devices* **2018**, *65*, 431–439. [[CrossRef](#)]
46. d’Alessandro, V.; Catalano, A.P.; Scognamiglio, C.; Müller, M.; Schröter, M.; Zampardi, P.J.; Codecasa, L. Experimental determination, modeling, and simulation of nonlinear thermal effects in bipolar transistors under static conditions: A critical review and update. *Energies* **2022**, *15*, 5457. [[CrossRef](#)]
47. Walkey, D.J.; Smy, T.J.; Macelwee, T.; Maliepaard, M. Compact representation of temperature and power dependence of thermal resistance in Si, InP and GaAs substrate devices using linear models. *Solid-State Electron.* **2002**, *46*, 819–826. [[CrossRef](#)]
48. Zhang, Q.M.; Hu, H.; Sitch, J.; SurrIDGE, R.K.; Xu, J.M. A new large signal HBT model. *IEEE Trans. Microw. Theory Technol.* **1996**, *44*, 2001–2009. [[CrossRef](#)]
49. Miller, S.L. Ionization rates for holes and electrons in silicon. *Phys. Rev.* **1957**, *105*, 1246–1249. [[CrossRef](#)]
50. Sasso, G.; Costagliola, M.; Rinaldi, N. Avalanche multiplication and pinch-in models for simulating electrical instability effects in SiGe HBTs. *Microelectron. Reliab.* **2010**, *50*, 1577–1580. [[CrossRef](#)]
51. d’Alessandro, V.; Schröter, M. On the modeling of the avalanche multiplication coefficient in SiGe HBTs. *IEEE Trans. Electron Devices* **2019**, *66*, 2472–2482. [[CrossRef](#)]
52. Nenadović, N.; d’Alessandro, V.; La Spina, L.; Rinaldi, N.; Nanver, L.K. Restabilizing mechanisms after the onset of thermal instability in bipolar transistors. *IEEE Trans. Electron Devices* **2006**, *53*, 643–653. [[CrossRef](#)]
53. Paasschens, J.C.J.; Harmsma, S.; van der Toorn, R. Dependence of thermal resistance on ambient and actual temperature. In Proceedings of the IEEE Bipolar/BiCMOS Circuits and Technology Meeting (BCTM), Montreal, QC, Canada, 12–14 September 2004; pp. 96–99.
54. COMSOL Multiphysics User’s Guide, Release 5.2A. 2016. Available online: <https://www.comsol.it/> (accessed on 1 August 2020).
55. PSPICE User’s Manual, Cadence OrCAD 16.5. 2011. Available online: <https://www.orcad.com/> (accessed on 1 August 2020).
56. Russo, S.; d’Alessandro, V.; La Spina, L.; Rinaldi, N.; Nanver, L.K. Evaluating the self-heating thermal resistance of bipolar transistors by DC measurements: A critical review and update. In Proceedings of the IEEE Bipolar/BiCMOS Circuits and Technology Meeting (BCTM), Capri, Italy, 12–14 October 2009; pp. 95–98.
57. Raya, C.; Ardouin, B.; Huszka, Z. Improving parasitic emitter resistance determination methods for advanced SiGe:C HBT transistors. In Proceedings of the IEEE Bipolar/BiCMOS Circuits and Technology Meeting (BCTM), Atlanta, GA, USA, 9–11 October 2011.
58. Krause, J.; Schröter, M. Methods for determining the emitter resistance in SiGe HBTs: A review and an evaluation across technology generations. *IEEE Trans. Electron Devices* **2015**, *62*, 1363–1374. [[CrossRef](#)]
59. PathWave Advanced Design System (ADS). 2022. Available online: <https://www.keysight.com/zz/en/lib/resources/software-releases/pathwave-advanced-design-system-ads-2022.html> (accessed on 1 August 2022).
60. AgilentHBT Model (Agilent Heterojunction Bipolar Transistor Model). Available online: <https://edadocs.software.keysight.com/pages/viewpage.action?pageId=6262855> (accessed on 1 August 2022).

61. Schröter, M.; Chakravorty, A. *Compact Hierarchical Bipolar Transistor Modeling with HICUM*; World Scientific Publishing: Singapore, 2010.
62. Sparkes, J.J. Voltage feedback and thermal resistance in junction transistors. *Proc. IRE* **1958**, *46*, 1305–1306.

**Disclaimer/Publisher's Note:** The statements, opinions and data contained in all publications are solely those of the individual author(s) and contributor(s) and not of MDPI and/or the editor(s). MDPI and/or the editor(s) disclaim responsibility for any injury to people or property resulting from any ideas, methods, instructions or products referred to in the content.